Chapter

Ceria as an Efficient Nanocatalyst for Organic Transformations

Farha Naaz, Umar Farooq and Tokeer Ahmad

Abstract

Valuable chemicals, fuels and pharmaceuticals obtained by the transformation of raw materials have fascinated a lot of researchers in past few decades. However, to reduce problems related to these transformations different green, sustainable and economic techniques have been developed to carry out such organic transformations. Development of nanostructured catalysts has been preferred to accomplish heterogeneous catalytic organic transformations because of greater number of surface-active sites for catalytic processes, high catalyst recovery rate, environment friendly nature and their ease of synthesis. Besides the advances in nanocatalysis, certain challenges including not well-defined morphologies due to loss of control over it and loss of catalytic activity during operation need to be addressed. Ceria is actively investigated in field of catalysis. As a ubiquitous component in catalytic system, its inception is like an irreplaceable component in organic transformations. In this chapter, we appropriately reported various fabricating approaches to synthesize Cerium and CeO_2-rooted nanoparticles and cerium nanoparticles supported on various support materials, accompanied with multimetallic schemes that show notable contribution to the field of catalysis. This comprehensive chapter will provide an improved understanding of nanostructured CeO_2 and will provide deeper insight in the catalysis of Ce-based nanostructured materials and further widen their ambit of applications.

Keywords: ceria, metal oxide, synthesis, nanocatalysis, organic transformations

1. Introduction

Deterioration of environment by excessive dependency on fossil fuel reservoirs encounters an array of challenges for our ecological system. Presently, some other practices such as producing harmful pharmaceuticals, hazardous by-products in manufacturing, etc., results in the severe environmental problems [1]. To encounter these challenges catalysts are needed, but their multiplicity and complexity demand a breakthrough in the approaches in which these catalysts are designed and used [2]. In chemical reactions, catalysts act as unsung heroes which have marked impact on human society [3]. By approaching recent catalytic constituents, moving beyond simple modifications and making efforts to understand the elementary principles, it has been made possible to synthesize and choose suitable catalysts for a provided set of reactants to obtain desired products [4]. These challenges can be resolved by utilizing various techniques like computational modeling, atomic resolution

microscopy and atomic scale measurements [5]. With the enhancements in chemical sciences, the property which is named as catalysis adorns the chemical reactions in appropriate aspects. Discussions regarding differentiation between homogeneous and heterogeneous catalysts have dominated research in the recent years [6–8]. Therefore, in this chapter we explore novel catalytic systems, which fulfill the specifications of both homogeneous and heterogeneous catalysts like higher activity and better reproducibility.

At this point, nano catalysis comes into the picture and dramatically shaped queries on combining the properties of both the catalytic systems in recent years. As considering nanodimensions, nanocatalysts possess high surface area which provide a better surface to reactants and this property resembles to homogeneous catalysis. The catalyst can act like heterogeneous due to the insolubility in the reaction solvent and hence carried out an adequate separation from the reaction mixture. In view of these significances, nanocatalysts has propelled to the forefront in investigations in recent years. Much attention has been drawn to explore a lot in the field of nanocatalysis and synthesis of nanomaterials for organic transformations. This encourages researchers to develop a simple, efficient, mild, environmentally benign, ligand free, heterogeneous, and reusable nanocatalyst for organic transformations [6]. Prior research has thoroughly investigated nanoscale catalysts in several reactions [9]. It has been recently studied that due to the high surface area and high activity, nanoparticles (NPs) find much importance in catalysis.

Rare earth metals and their complexes exhibit rich variety of solid-state properties and characteristic behavior which make them interesting subjects for catalyzing many organic transformations. There are 14 lanthanides included in the rare earths which include yttrium and scandium also. Among all the rare earths, several researchers corroborate cerium in the field of catalysis. The abundance of cerium in the upper crust is 64 ppm which is relatively higher than copper, tin and any other rare earth elements. Nanoceria has been regarded as the potential catalyst by employing under ligand free conditions in the form of metal, metal oxides for various organic reactions. Cerium due to its outstanding catalytic efficiency and enough abundance makes it useable for a variety of reactions which makes it the selective element for validating the catalytic conversion of the exhaust system of automobiles in automotive industry [10]. Several studies carried out have revealed that due to the high surface area and reactive morphologies of ceria-based nanomaterials can be effectively used as catalysts for organic transformation reactions such as oxidation, reduction, hydrogenation, coupling reactions and many more [11–13] as represented in **Figure 1**. The rare earth elements occur in many minerals inside the earth's crust with quite higher abundance. Being actively investigated, cerium oxide is most imperative and well-known among light rare earth oxides, especially its use in catalysis [14]. Jons Jakob Berzelius and Wilhelm Hisinger were first who discovered elemental cerium in 1803. The exact values of crustal abundance of cerium (average concentration in the earth's crust) are still contentious. For instance, Kleber and Love stated 46 ppm for the cerium crustal abundance in 1963, while Jackson and Christiansen reported the value of 70 ppm in 1993; McGill reported a wide range from 20 to 46 ppm in 1997. Lide reported the value of 66.5 ppm in 1997, representing the intermediate of the various reported values, was commonly accepted for present discussions [15]. Light rare-earth metals occur mainly in the minerals of fluorocarbonate form called bastnasite and phosphate form called monazite. The elemental distribution varies in both minerals and locations. In bastnasite, cerium content is 49.1% with respect to all the rare earth content from Mountain Pass, California, U.S.; while the content is 50.0% located in

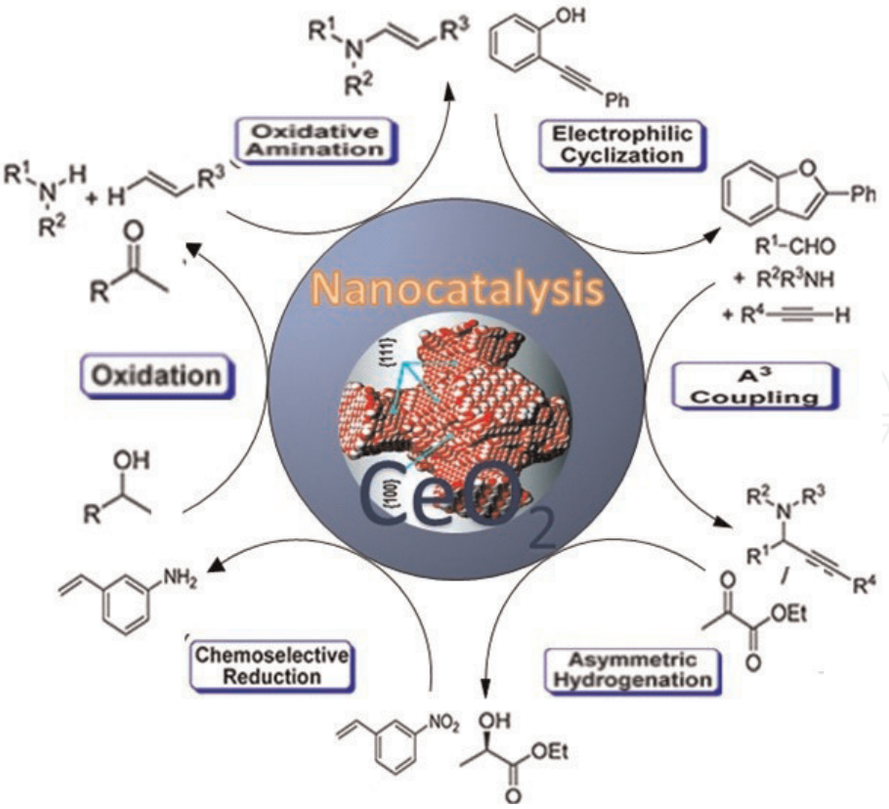

Figure 1.
Nanostructured ceria catalyzed organic transformations.

Bayan Obo, Inner Mongolia, China. The cerium content is 45.8% in monazite minerals at North Staradbroke, Australia and 47% in East Coast Brazil [16]. In the lanthanide group, Cerium is an element with an atomic number of 58. Cerium often shows +3 oxidation state, where it acts as typical rare earth and it also exceptionally has a stable +4 oxidation state.

Metallic cerium, $Ce(OH)_3$ and other oxosalts of cerium like oxalate, nitrate allowed to heat in air or oxygen for the production of its oxide form, i.e., cerium (IV) oxide (CeO_2) [17]. CeO_2 is a well-known cerium compound which is pale yellow/white powder synthesized by cerium oxosalts calcination and generally used as a catalyst or as three-way catalysts (TWCs). The ceria with fluorite structure has tetrahedral holes with oxide ions residing within it, which are formed by the face-centered cubic array of cerium ions, and vacancies are at the octahedral holes. Each cerium ion equivalently surrounded by eight oxygen anions and four cerium cations are tetrahedrally coordinated to these anions. The lattice constant of each unit cell is 5.411 Å. These eight coordination sites are occupied by a cerium cation. It is determined that its structure possess large vacant octahedral holes which intensify its further applications. Ce(III) trioxide (Ce_2O_3) also occurs under ambient conditions [18]. Ce_2O_3 is very unstable against oxidation and as a pressure of 10–40 atm of oxygen is applied, it gets oxidized and then CeO_2 begins to form. Characterization techniques such as X-ray diffraction studied at different temperatures reveals that Cerium oxide have also been observed in other phases. For example, a disordered non-stoichiometric fluorite-related phase of α-phase cerium oxide, is stable above 685°C (CeOx, $1.714 < x < 2$) [19, 20]. A β-phase formed at room temperature with a rhombohedral structure (CeOx, $1.805 < x < 1.812$) remains stable until 400°C [21, 22].

Over the last years, cerium's price has continually dropped as compared to the other rare earth elements. Although fascinating, the cost of cerium oxide cost is going below the price of lanthanum oxide and has observed a sheer incline in its application. CeO_2 has been focused for a plethora of studies both in industry and in academia [23].

2014 and 2015 are the most profused years which have recorded about 2300 publications related to ceria materials. It must be because 1301 publications on catalytic applications in 2015 mark a booming interest in ceria catalysis for the first time become 50% of the total [24–30]. Though, it is worthy to reveal the number of studies on the utilization of ceria in new scientific areas such as biology and pharmaceuticals. Ceria has been used as a support for stem cells cultured in vitro [31] or as a vehicle for intracellular drug delivery [32]. One more noteworthy study reveals that ceria nanoparticles could treat ischemia as well as reduce ischemic brain damage by interruption of the blood-brain barrier after ischemia [33]. Even more fascinatingly, the thermal water and CO_2 splitting by the employment of CeO_2 in solar reactors for fuel generations has been evolving as a novel and exciting investigation topic while accumulation of ceria-based compounds in photocatalysis which merits special mention is another rising field [34, 35].

2. Structure and morphology affecting the catalytic properties of ceria

Structure and morphology play a key role in determining the application of the material by influencing its surface properties. Extensive studies have been conducted to unveil different applications which depend on morphology of nanocrystals. The crystal plane is one of the most common morphological parameters being considered in cerium oxide crystals. The surface of materials is important in various physical and chemical processes that involve the reaction on inorganic oxides such as catalysis and crystallization [29]. CeO_2 in cubic fluorite structure possesses three low-index planes: (100), (110) and (111) as shown in **Figure 2**. The (100) planes contain scattered charged planes which establish a dipole moment perpendicular to the surfaces which are not stable. However, they could be sustained by charge-counteracting species for example, ligands or surfactants or by defects present. The (110) surfaces are charge neutral which consists of anions and cations in stoichiometric proportions in each plane, which exhibit negligible dipole moment perpendicular to the surface. The (111) surfaces also results no dipole moment perpendicular to the surface. Unlike the (110) planes, (111) surfaces consist of a neutral three-plane replicating subdivision ended with a single anion plane. The (100) facet exhibits 2.0 eV of surface energy, the highest one among these three low-index facets and the (111) plane is calculated as the most stable facet irrespective of different potentials used in simulation, both before and after relaxation according to the work done by Vyas. While (110) plane is the other highly stable facet, comprising a surface energy of 1.5 eV from Butler potential calculation [36]. Hence, different shapes of nanostructured ceria particles have different crystal surfaces and plane properties, which further enhances their performances in different systems including catalysis by affecting the interactions between the ceria surface and adsorbed molecules. Fronzi et al. stated similar results on the three low-index surfaces of CeO_2 as they performed density functional theory (DFT) investigations. The stoichiometric (111) surface is the most stable surface structure with a surface free energy of 0.060 eV under oxygen rich conditions calculated by "ab initio atomistic thermodynamics." The subsurface oxygen vacancies of (111) surface has been found to be the most stable one with a surface free energy of -0.001 eV/Å^2 in a reducing environment. While in a highly reducing environment,

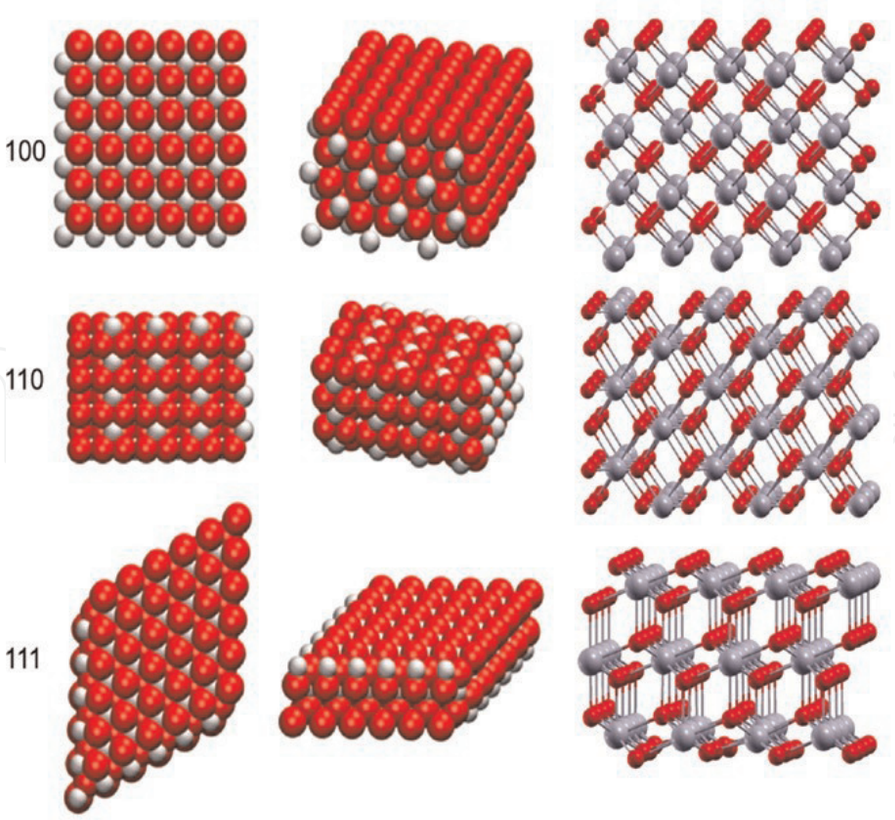

Figure 2.
Diagrammatic representation of CeO_2 facets (100), (110), and (111). Cerium and oxygen ions are represented by red and gray spheres. Reprinted with permission from Ref. [42]. Copyright 2017 American Chemical Society.

a Ce-terminated (111) surface is the most stable one. CeO_2 (110) surface with surface oxygen vacancies has 0.012 eV/Å^2 surface free energy, which is 0.006 eV higher than CeO_2 (111) surface with same oxygen vacancies. The surface free energies of CeO_2 (100) surface having the same type and amount of surface oxygen vacancies terminated with oxygen and cerium are 0.575 and 0.016 eV/Å^2 respectively, which are both larger than those of CeO_2 (111) and CeO_2 (110) surface [37]. Sayle and coworkers reported the surface energies of 11.577 and 2.475 J/m^2 for (331) planes before and after relaxation through applying energy minimization code MIDAS [38]. Other crystal planes of cerium oxides, such as (200), (220), (331) planes, etc., have also been investigated and characterized in both experimental and simulation studies [10, 13]. For example, {220} facets were found in a slightly truncated cerium oxide nanocubes with predominate (100) facets synthesized by Kaneko et al. [39, 40]. Moreover, the feasibility of tailoring the metal oxide morphology have upgraded due to recent advancements in materials chemistry, and the required crystal planes of the cerium oxide materials can be favorably exposed through precise control of the growth kinetics. However, these three low-index planes are the most commonly observed and the most studied facets on synthesized cerium oxide structures [30, 41, 42]. It is also reported that perception about the nanocatalysis must be explained by intrinsic properties of nanoparticles which include (**Figure 3**) (i) quantities such as bond length and binding energy; (ii) quantities related to cohesive energy per discrete atom and the activation energy for atomic dislocation and diffusion, etc.; (iii) properties such as the Hamiltonian which demonstrate band structure, band gap and (iv) properties from the combined effect of binding energy density and atomic cohesive energy like surface area, surface strength, etc. [43].

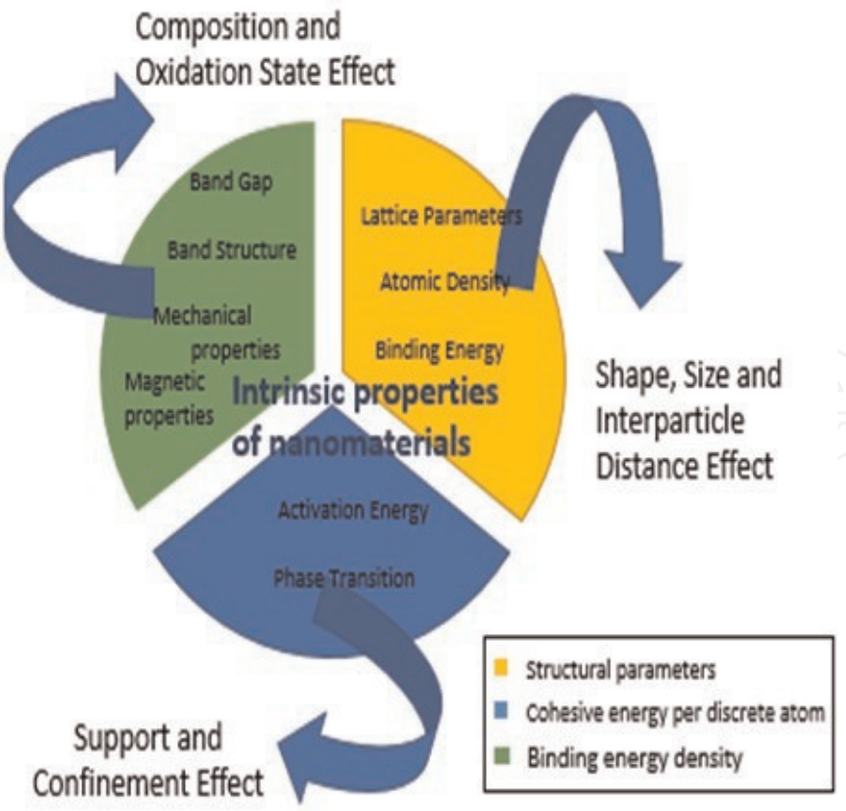

Figure 3.
Intrinsic properties affecting catalytic activity of nanomaterials.

2.1 Mechanism of reactivity and catalytic activity of ceria

In the growing field of catalysis, ceria attributed oxygen storage capacity (OSC) as its fortune. CeO_2 shows multi valence nature which give large number of oxygen vacancies to produce under stoichiometric CeO_2-x at reducing temperatures, which can be oxidized back to CeO_2 in an atmosphere containing oxygen. As cerium (III) (Ce^{3+}) switches to cerium (IV) (Ce^{4+}) states, it results in high oxygen mobility in the ceria lattice that in turn leads to a strong catalytic potential and it happens without any structural modification of the fluorite ceria lattice. The change in energy can cause largely a surface effect to heterogeneous catalyst [44–46].

Thus, scientists have been looking for maximizing the formation of oxygen vacancies of ceria-based catalysts to improve their activity, which needs high temperatures and a reducing atmosphere. Yan's group had made the first observation during the study of preparation of ceria nanostructures, which depict that as compared to octahedral ceria nanoparticles, nanocubes and nanorods had a higher capacity to store and release oxygen at high temperature. Recently, the precise fabrication of functional nanostructured ceria is turn out a routine. Though, some other materials also demonstrate very discrete catalytic activity due to defect sites effect and exposed crystal facet, even from materials which have similar structures [16, 47–51]. The values which are reported in **Table 1** display the exposure of {100} and {110} planes in nano-size ceria accompanying the improved oxygen storage capacity (OSC) and show the following order of OSC nanocubes > nanorods ≫ nanopolyhedra [41]. An appropriate comparison is done with determined hypothetical surface area-normalized OSC which is calculated on more reducible surfaces and specify that OSC is not only defined to the surface, but it also takes place in the bulk [52]. On introduction of defects into the lattice, it is investigated that through controlling synthetic and postproduction parameters, preferred crystal

	OSC[a] (μmol O/g)	OSC/B.E. T (μmol O/m^2)	Calcd OSC[b] (μmol O/m^2)
Nanopolyhedra	318	5.1	6.2
Nanorods	554	9.1	4.9
Nanocubes	353	10.6	5.7

Reprinted with permission from Ref. [41]. Copyright 2005 American Chemical Society.
[a]CO-OSC measured at 400°C.
[b]Calculated according to the theoretical OSC of exposed surfaces. See Ref. [41] for details.

Table 1.
Oxygen storage capacity of variable nanostructures.

orientation is précised. It is also noticed that the reactivity of the surface of crystal is greatly affected by variable lattice defects critically.

Vacancies included in the lattice defects are (a) oxygen vacancy defects, (b) self-interstitials, (c) interstitial impurity atoms and (d) edge dislocations [53]. In the fluorite lattice of ceria, the degree of oxygen mobility accredited to its size, dispersion, and value of oxygen vacancy defects (OVD) [54–57]. The empty 4f states of cerium located electrons by surrounding a vacancy in the ceria support lattice establishes defect sites [17, 58–61]. These defects are shown to be mobile with high oxygen mobility and arise around cerium (III) ions only. On introducing subsurface vacancies into the lattice, the mobility of the vacancies, and therefore the defects, is decreased significantly. The formation of vacancy clusters is in the three or six surrounding cerium ions of the material's surface. An oxygen vacancy defect tends to form under low partial pressure of oxygen [17]. After approaching a favorable oxygen by another oxygen, a bond is formed, and from the surface of the crystal the oxygen molecule can diffuse away. Respectively, the oxygen molecule that is obtained, further diffuses away from the surface and two electrons are left back to be distributed between three cerium atoms. Due to this, cerium atoms undergo partial reduction to a valency between the 3+ and 4+ states. It occurs in a manner to leave behind triads of vacancies which are surrounded by nine cerium atoms sharing eight electrons [62–65]. It is widely proposed that change in the adsorption energy regarding carbon monoxide and oxygen can cause the change in activity of a surface with lattice strain. It is noteworthy that the similar researches reported a lesser increment in the adsorption energy related to carbon dioxide [66, 67]. The adsorption energy for oxygen is about five times superior than for carbon monoxide. Furthermore, the activation barriers respecting to dissociation of oxygen and formation of carbon dioxide are greatly dropped. However, the ease of formation of the oxygen vacancies facilitate the reaction. A molecule of carbon monoxide adsorbs on the surface of the ceria and readily reacts with oxygen existing on its surface and further diffuses away in the form of carbon dioxide leaving an oxygen vacancy. This oxygen vacancy results in a weakened bond between the oxygen atoms, as it allows an adsorbed oxygen molecule to react with the surface. Across the surface of the catalyst, a carbon monoxide diffuses until it encounters the excess oxygen and diffuses away from the surface [68–71].

2.2 Nanoarchitectured ceria and its influence in the behavior to supported metals

The vast expansion of the usage of the nanomaterials offer is just incredible. Nanotechnology revolution has revolutionized the research arena as matter of the fact that it creates the vast possibilities to fabricate the materials with nanodimensions. Catalysis, fuels and microelectronics are different fields of

applications where nanostructured cerium oxides grow rapidly and reflecting their importance in enhancing the performances of those systems. Variable morphologies of ceria nanoconstructs have been explored in these applications, for instances nanocubes, nanorods, octahedron polyhedron, tube and many more. Ceria nanostructures with various shapes possess the different crystal planes and surface morphologies, which influences the interactions between the ceria surface and adsorbed molecules, and hence changes the performances in different systems. Zhou et al. described many strategies for synthesis of well-controlled morphologies of nanostructured ceria. Now, Ce-based materials with controlled morphologies which exhibit zero-, one-, two-, and three-dimensional structures are possibly synthesized. (**Figure 4**). The categories defined on basis of number of dimensions which cannot be restricted to the nano-range (<100 nm).

Nanostructured ceria with Zero-dimensional (0D) possessing isotropic cubic phase of the fluorite structure can be observed distinctively. According to results, it presented a lack of fortunate growth direction of seeding crystals. Hence, (0D) nanostructures have most straightforward synthesis. Mono-dimensional (1D) CeO_2 nanoparticles possess the different properties due to which they have been explored more than the 2D and 3D architectures and a variety of synthesis procedures were proposed. 1D hexagonal Ce_2O nano-rods (NRs) synthesized by template-free electrochemical growth method on a Ti substrate which mainly exposes the {110} planes and displayed outstanding photocatalytic activity in hydrogen evolution, with H_2 yield reaching 741 mmol g^{-1} [26].

The preparation of 2D and 3D architectures are drawing significant attention and they also evolving as good alternatives in various catalytic and energy applications. For the construction of a spongy mesoporous CeO_2 microspheres an analogous concept was assumed in which in-situ formation of the removable template by graft polymerization reaction between acrylamide and glucose takes place [72]. Ceria nanocubes synthesis is important because their possession of high surface energies usually exhibit specific activities due to the unsaturated coordination atoms, atomic steps and ledges [73–75]. Numerous fabrication methods have been reported for spherical nanostructures [76–79]. Planes in ceria octahedron have gained much attention as these planes are exposed on their surfaces [80]. Nanostructured ceria with different morphologies, such as nanotubes, spindles, nanosheets, etc. have been synthesized [45, 80, 81]. Due to their enormously developed activities ceria nanorods have increased wide-ranging interest than those of ceria with other shapes in many different reactions, such as CO oxidation, NO reductions and 1,2-dichloroethane and ethyl acetate oxidation [57, 82, 83]. By means of the most stable (111) planes on the surface, ceria octahedra demonstrated the least catalytic activity being studied when compared to the activities of nanocubes, nanorods and other shapes in many reactions, such as CO oxidation and ethyl acetate oxidation [80, 83], Notable progress has been made to achieve these

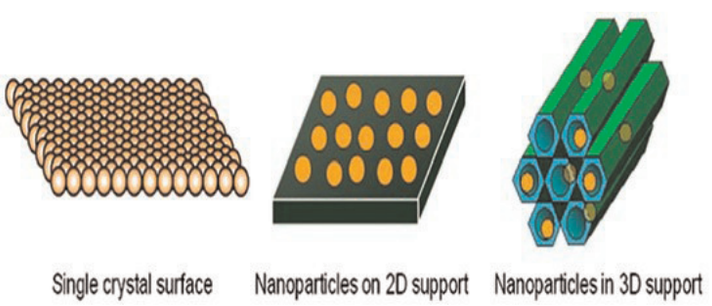

Figure 4.
1D, 2D and 3D nanostructures. Reprinted with permission from Ref. [2]. Copyright 2010 Springer Nature.

ceria nanomaterials. However, synthesizing these morphologically different nanostructures with well-controlled size and homogeneity is still difficult due to their uncommon shapes. For instance, it is difficult to prepare nanosheets due to their exceptionally small thickness and possible quantum size effects [84].

In Prospect, the synthesis of ceria NPs requires the interaction with metal nanoparticles that act as the "active sites" for catalysis. Schelter and co-workers reported a ligand to vary the stability of the Ce (III)/Ce (IV) redox couple, in their synthesized 1,3-bis [(20 tertbutyl) hydroxyamino phenyl]-benzene Ce complex, [85]. Recently, a hydrothermal process has been used for the synthesis of Au@CeO_2, presenting core-shell systems grounded on other precious metal core-shell [86], while Ag@CeO_2 was also synthesized by reverse micelle/redox reaction [86–90]. Among different characterization, an exclusive strength of the STM technique is the ability to enquire the atomic structure of surfaces, down to the level of distinct defects and adsorbates. **Figure 5** shows one such image, obtained on the surface of a CeO_2 (111)/Pt (111) system [91].

Catalytic characteristics of supported metal nanoparticles depend on the role of the support as well as on the composition, shape, particle size, and chemical state too. The catalytic reactivity is directly related to the atomic interaction within support and metal nanoparticles which is termed as metal-support interaction which has attained significant attention nowadays (**Figure 6**). Due to the possession of unique properties by the ceria by virtue of which it makes oxygen species readily available to the metal site which make its outstanding applications in large number of catalytic reactions. This way, noble metals on ceria are activated for various oxidation reactions at low temperatures [92].

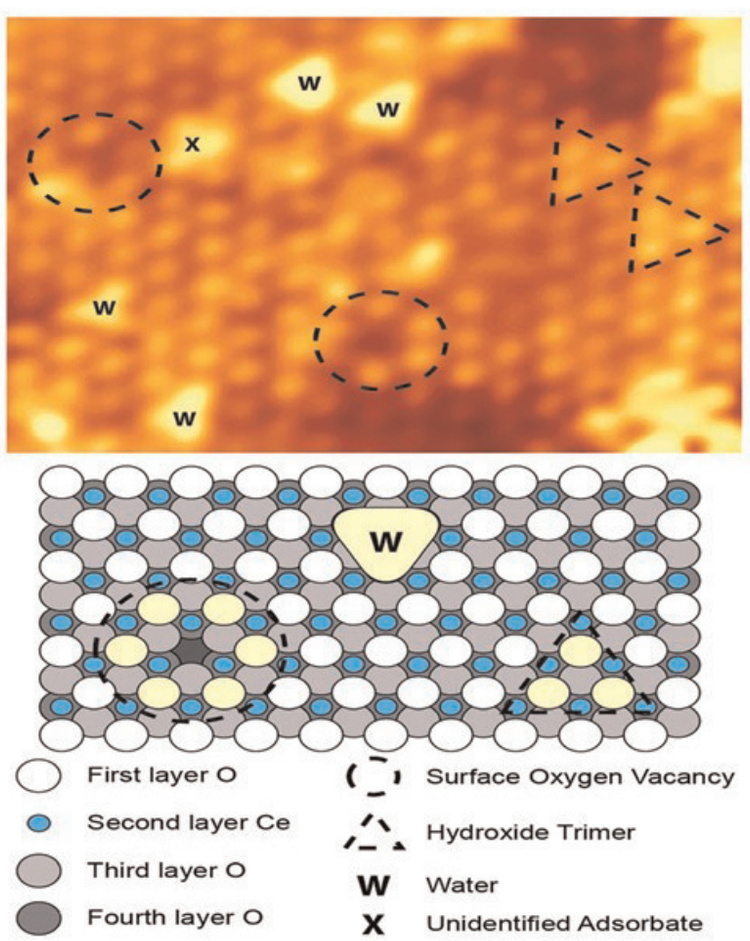

Figure 5.
STM image of the CeO_2 (111)/Pt (111). Reprinted with permission from Ref. [91]. Copyright 2010 American Chemical Society.

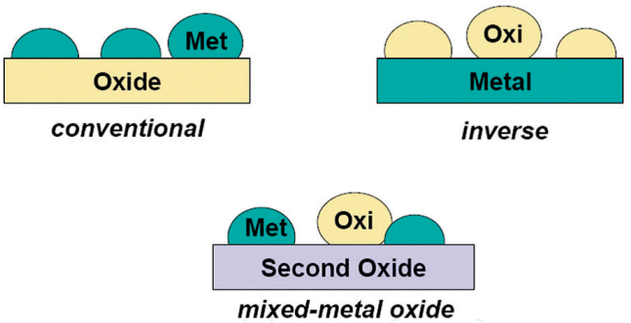

Figure 6.
Metal-oxide configurations used in studies with ceria model catalysts. Reprinted with permission from Ref. [92]. Copyright 2017 Royal Society of Chemistry.

A pivotal role is played in the activity of catalysts by the nature of their support. Vayssilov et al. has studied the origin of interactions proposed between the various support effects like the active (metal) phase and support which include interaction of electrons among both components [93], destabilization or stabilization of particle sizes or shapes [94], surface transport of adsorbates through the boundary (spill-over, reverse spillover capture zone effects); [95] and the stabilization/destabilization of oxidized active phases by the support or strong "metal-support interactions" relating movement of partially reduced oxides onto the active phase [96–98]. The metal oxide intervenes in the catalytic process as well as an inert support [99].

Pure ceria, CeO_2, undergo degradation with time at elevated temperatures which minimize its performance due to reduction in its surface area as well as oxygen storage capacity (OSC), also it has been presented that pure ceria accommodate "active" weakly bound oxygen species, which relates bulk rather than to the surface by using steady-state CO oxidation kinetics and/or temperature-programmed desorption (TPD) [100–102]. Thus, development of CeO_2 based nanocatalysts for chosen activities is surely done with a keen understanding about metal-ceria support interaction in supported metal catalysts (**Figure** 7). E. Mamontov used pulsed neutron diffraction to investigate the nature of these "active" oxygen species in pure ceria. The study of oxygen position in oxides by neutron diffraction demonstrates a comparable scattering contrast of oxygen and metal ions. In the real space the oxygen defects in CeO_2 examined by both pulsed neutron diffraction data and atomic pair-distribution function (PDF) analysis whereas in the reciprocal space, it is analyzed by the Rietveld refinement [103].

Zirconia, ZrO_2, has been actively investigated in many studies and have been characterized. The enhanced OSC of ceria-zirconia related to ceria as well as known to improve partial degradation of ceria at high temperatures. It is also probable that

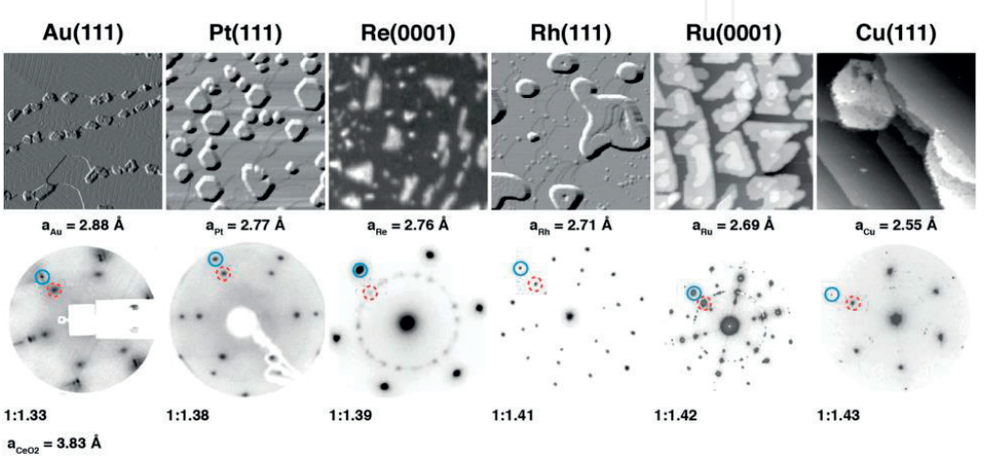

Figure 7.
Real (STM, LEEM) and reciprocal space (LEED) of ceria structures on a range of metals. Reprinted with permission from Ref. [112]. Copyright 2016 American Chemical Society.

the necessary oxygen mobility which is essential for the functioning of CeO_2 as a catalytic support is provided by the interstitial oxygen ions which act as "active" sites [104–111].

CeO_2 impart high oxygen storage and release capacity and it is predicted as the finest supporting material for catalysis at Au NPs following other properties such as facile oxygen vacancy formation, and narrow Ce f-band. Au gets oxidized once in contact with CeO_2. The atomic and electronic interaction between reduced CeO_2 and supported Au NPs is highly contributed by the electrons located on the occupied 4f-orbital of Ce^{3+} ions. Ceria particles were also deposited on the surfaces of Au, Pt, Re, Rh, Ru, Cu to produce inverse oxide/metal catalysts and these supports can cause dramatic effect on the structure of ceria islands in an inverse catalyst [112, 113]. The electron transfer is induced from metal to the support because of the presence of platinum over ceria nanoparticles leading to the formation of a small fraction of Ce^{3+} cations. Among transition metal core-Pt shell nanoparticles, altering Au NPs with alloying elements would be an interesting strategy for lowering CO adsorption energy, as well as deducing and enhancing saturated CO and O_2 concentration, correspondingly. Vayssilov et al. studied that a crystalline atomic arrangement exhibited by the interaction of an illustrative metal cluster Pt8 with two group of model ceria nanostructures [114]. A Pt8 cluster was selected as a model which supported on a stoichiometric $Ce_{40}O_{80}$ nanoparticle. The metal group relates five Pt atoms with ceria particle found as most stable structure for Pt8/$Ce_{40}O_{80}$. Liu and colleagues [115] prophesied adsorption and dissociation of oxygen and transport processes on the two most stable Ag (111) and Ag (110) surfaces and reveals a binding energy of CeO_2 catalysts and on a monolayer silver supported by CeO_2 (111) surfaces with or without oxygen vacancies by DFT with PAW method. The computed energies of these reactions display that the process of oxygen reduction and the combination of the dissociated oxygen ions in the oxide electrolyte prefer taking place in the triple phase boundaries (TPB) region with oxygen vacancies [116].

2.3 Synthesis and characterization of ceria nanoparticles

This segment of the chapter encompasses the detailed outline of various synthesis techniques and the conditions applied for the reaction which influences the final product. According to the applications in various fields, the synthesis of ceria nanoparticles with desired morphology is very important; therefore, thorough investigations were done by researchers to investigate several approaches. The studies on Ceria based nanoparticles demonstrated that conditional to the synthesis methodology, wide variations may occur in shape, size, crystal structure, and properties of nanostructures, as well as the physical and chemical conditions employed during the reaction process. Current literature revealed many chemical methods, such as, hydrothermal method, co-precipitation method, a micro emulsion mediated approach, and other methods like sol-gel synthesis have been employed to synthesize cerium based nanostructured materials.

Hydrothermal method refers to the oxide synthesis and crystal growth in aqueous solutions under high temperature and pressure using a sealed heated vessel which is known as autoclave. It is well-established method for the laboratory and industrial scale synthesis of nanoceria materials. Two big advantages of this method are that: the reaction temperature is below the melting point of reactants, and the operational parameters such as reaction temperature, duration, autoclave types can be easily tuned to modify the reactivity of synthesized inorganic solids [117].
A facile hydrothermal method for the synthesis of ceria nanocubes with six {100} facets using oleic acid as the surfactant was developed by Wang and co-workers. The as-prepared ceria was single crystalline, confirmed by uniform crystal lattice fringes. The sizes were well controlled with side lengths from 9 to 17 nm [92].

A single-step hydrothermal method is utilized in the fabrication of uniform CeO_2 nanoparticles with diameter approving nano-size, i.e., 13–17 nm and further, hexamethylenetetramine is added for the formation of (220)-dominated surface structure.

Co-precipitation synthetic method is another extensively used approach for preparing nanomaterial. The strategy is best choice for commercial synthesis of CeO_2 and due to very low solubility of ceria, it attains great advantage. This method is simple and rapid preparation process which makes it easy to synthesize controllable particle size and flexible in altering overall homogeneity of the particle with its surface state [118]. The cerium precursors are generally inorganic cerium salt, such as $Ce(NO_3)_3$, $CeCl_3$, $(NH_4)_2Ce\ (NO_3)_6$, and the precipitating agents are usually NaOH, NH_4OH, hydrazine and oxalic acid [119–122]. Abimanyu and coworkers performed co-precipitation method and applied ionic liquid as a template to prepare magnesium and cerium mixed oxides. To overcome the difficulty of controlling particle size, template-assisted co-precipitation, carbonate co-precipitation, redox co-precipitation, etc. have been presented in conventional co-precipitation method [118].

Sol-gel method is highly suitable for the fabrication of metal oxides (**Figure 8**). This method is widely used in ceramics industry and materials science for producing solid materials such as ceramic fibers and dense films. It is easy to accomplish and does not need any special conditions and equipment [117]. The process involves conversion of metal alkoxide/chloride solution into a colloidal suspension (sol) and gelation of the sol to form discrete particles or network polymers in a continuous liquid phase (gel) [123]. Gnanam et al. successfully prepared nanocrystalline cubic fluorite/bixbyite CeO_2 or α-Mn_2O_3 via simple sol-gel method using cerium (III) chloride/manganese (II) chloride as the precursor by using methanol as a solvent calcined at 400°C [124].

The reverse micelle technique offers the greatest control over size and morphology. It is a wet chemical method in which pools of water are enclosed by surfactant molecules in an excess volume of oil. During synthesis procedure, surfactant molecules retain particles separated and confine particle growth this keeps control on size and shape of particles. The root for the technique is the use of a surfactant to stabilize variable aqueous droplet sizes in hydrocarbon medium. Metal salt precursors are transformed by a reactant from the hydrocarbon phase and are contained in

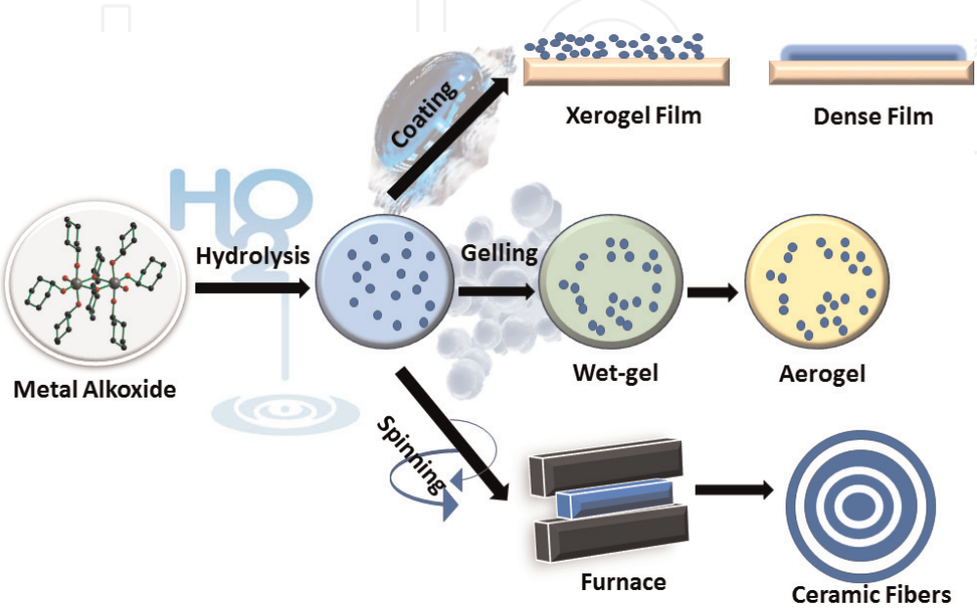

Figure 8.
Diagrammatic illustration of different stages of sol-gel method. Reprinted with permission from Ref. [118].

the aqueous portion. Mutually, the structure of the surfactant and the steric size can produce metals having a wide range of grain sizes. Masui et al. [125] synthesized ceria nanoparticles by using reverse micelles and reported fluctuation of bandgap values from 3.38 to 3.44. Ganguli et al. fabricated monophasic nanoshaped oxides by performing similar versatile methodology [126, 127].

The worth of morphology-activity association is clearly recognized with the implementation of different examples as breakthrough. With the advanced characterization techniques included SEM, HR-TEM, STM, uncountable studies investigated that morphology/exposed facet combination still contain some uncertainties and, so, on the mechanism of crystal growth. Some focus is also bounded by surface reactivity analysis or through TEM. The elucidation of this area is must to simplify instrumentation acquaintance [128, 129]. The powder XRD patterns of the CeO_2 nanorods, nanocubes and nanopolyhedra are of pure cubic phase shows its fluorite structure with lattice constants of 5.414(3), 5.436(3), and 5.405(3) Å, respectively (**Figure 9a**). The enlargement of the reflections indicated their nanocrystalline nature, recognized to the polyhedron and rods distinctly. The sharper reflections for cubes implied their larger sizes as compared with the former two samples. X-ray photoelectron spectroscopy (XPS) and X-ray absorption near edge spectroscopy (XANES) techniques investigate the oxidation state of cerium ions in ceria nanoparticles. The remark of the existence of the Ce^{3+}/Ce^{4+} shifts in150 mm active region leads to the inference that the lateral electron transport and surface reaction kinetics on the thin ceria electrodes are co-limiting processes. The XPS spectrum of the CeO_2 nanorods is shown in **Figure 9b**. It illustrates six consistent Ce 3d binding energy (BE) peaks for the rods with the former report on Ce^{4+}, signifying +4 was the main valence of rods in cerium [41]. The surface termination of oxide-based nanoparticles can be easily determined by the transmission electron microscopy (TEM) [130, 131]. The specific surfaces of catalytic CeO_2 nanostructures during a reversible beam induced redox reaction examined by combination of direct aberration corrected TEM and computational exit wavefunction restoration at ambient temperature.

Mesoporous ceria being versatile attracted researchers as catalysts and catalyst-support which possess increased dispersion of active secondary components and offer high surface area (**Figure 10**). Additionally, an issue which is mandatory to discuss is that as surfactant is removed during synthesis procedure, it shows its poor thermal stability at elevated temperatures precepted to be caused by collapsing of

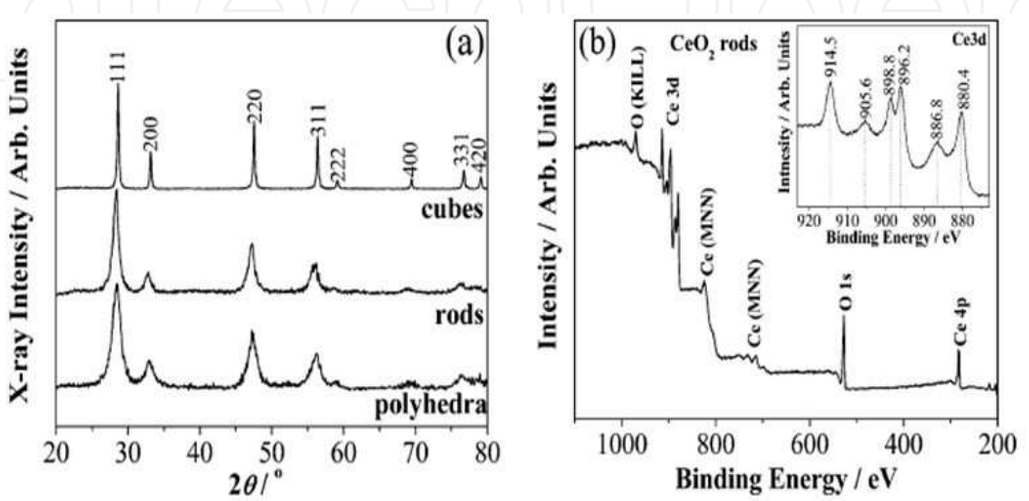

Figure 9.
(a) XRD patterns of CeO_2 nanorods, nanocubes and nanopolyhedra and (b) XPS wide spectrum of the CeO_2 nanorods. Reprinted with permission from Ref. [41]. Copyright 2005 American Chemical Society.

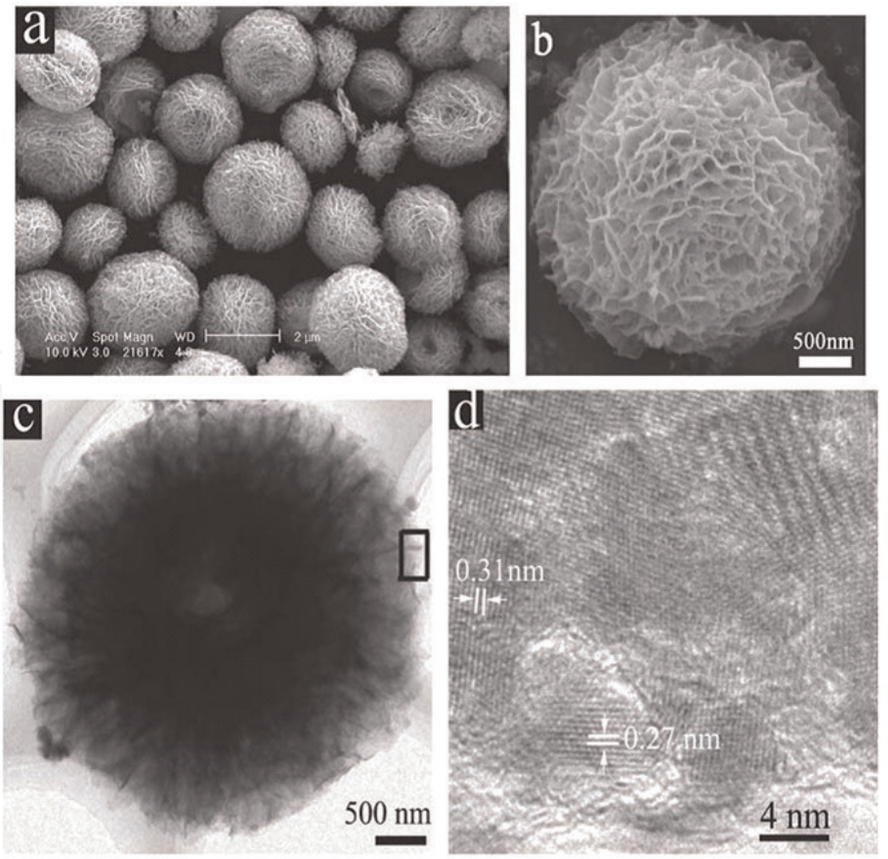

Figure 10.
Illustrative SEM images (a and b) and TEM images (c and d) of the flowerlike CeO_2 microspheres. Reprinted with permission from Ref. [72]. Copyright 2006 American Chemical Society.

structure. So, mesoporous CeO_2 has been developed by a novel hydrothermal method for high performance catalysts with excellent thermal stability [72, 132–135]. Hojo et al. analyze cationic reconstruction by using in-situ phase contrast HR-TEM with spherical aberration correction [136]. STEM, EELS, and theoretical calculations were performed to inspect the atomic structure of grain boundary which is selected as a model grain boundary in thin films of CeO_2 [38, 137, 138].

2.4 Cerium oxide catalyzed organic transformations

Organic synthesis occupied one of the most protruding places in the field of chemistry research. Additionally, the space of organocatalytic reactions is well-reviewed and widely examined. Further, initiating with certain reports to describe the organocatalytic applications of ceria nanostructures. Investigations on CeO_2 as catalytic support or recently as catalyst for conversions in organic reactions are liberated in accumulated manner. Although, the versatile behavior of this material is selectively observed in various catalytic applications. By Mars-van Krevelen mechanism, computer stimulation techniques were performed to predict the higher reactivity of ceria {110} and {100} surfaces towards carbon monoxide oxidation, which stated that CO first interacts with surface ceria oxygen and produce CO_2 by leaving an oxygen vacancy which is then filled with gas phase oxygen [139, 140]. The CO oxidation frequency turnover is higher on {110} as compare to {100} and {111} surfaces, presented as the opposite order of oxygen vacancy formation energy. CeO_2–ZnO composite catalyst utilized in hydrogen transfer reaction by Mishra et al. for cyclohexanone with isopropanol and it showed 51.3 mol% conversion of cyclohexanone [82]. Acetalization of cyclohexanone with methanol also reported by Rose

et al. using different transition metals [141]. Tamizhdurai synthesized CeO_2 and inspect it with various spectroscopic and analytical techniques. Afterwards, its oxidation effect was investigated on benzyl alcohol which reveals better conversion and selectivity. The catalytic oxidation properties of ceria closely tied with its redox and oxygen storage behavior, and CO oxidation can work as a model reaction to probe the redox properties of CeO_2 [142] (**Scheme 1**).

Zhou et al. [143] explored oxidation of carbon monoxide over ceria nanostructures in their study where they compared nanorods and irregular nanoparticles of same surface area; the former attributed exposed planes of {100} and {110} surfaces with higher proportion has higher activity. This study initiated the investigation of CO oxidation with nanoparticles, and several investigations were followed which clearly establish the correlation between ceria shapes and CO oxidation as shown in **Figure 11** [143–150]. CeO_2 nanospheres fabricated sonochemically in 1-butyl-3-methylimidazolium bis(trifluoromethylsulfonyl)imide [C4mim] [Tf2N] show the best presentation for low-temperature CO oxidation [151].

CeO_2 nanoparticles explored by Deori K. for the para-xylene oxidation to terephthalic acid as a heterogenous catalyst (**Scheme 2**). The synthesis procedure is environmentally friendly, and water was used as a solvent during catalysis reaction. The ceria nanostructures which were synthesized acquire 15 nm sized particles and high surface area of 268 $m^2\ g^{-1}$ [152].

The advancement in catalytic performance of the cube shaped CeO_2 nanoparticles displayed by the conversion of benzyl alcohol (BA) and para-chlorobenzyl alcohol (PCBA) to their respective aldehydes (>99%) (**Schemes 3**). Accompanying, in toluene ($PhCH_3$) oxidation, this CeO_2 nanocube catalyst was found to be very effective, as well as being more effective than the nanorods. Besides, reusable property of CeO_2 nanocatalyst also proposed for several cycles which display obtainment of the desired products without any deterioration in selectivity and activity in all cases [153].

CeO_2 is actively used in hydrogenation reactions as a promoter or carrier of noble metal nanomaterials for many years [154, 155]. As compared to oxidation reaction on CeO_2, hydrogenation owing to the specific role of adjacent oxygen on

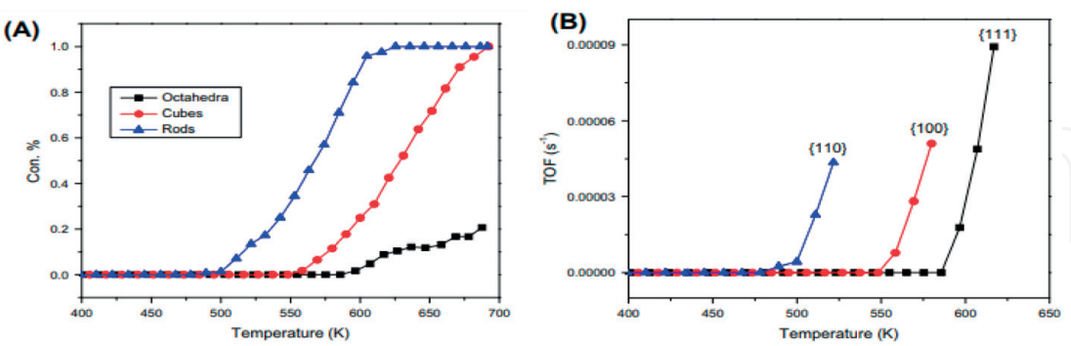

Figure 11.
(A) CO oxidation over ceria rods, cubes, and octahedra. (B) Comparison of CO turns over frequency oversurface planes (110), (100) and (111). Reprinted with permission from Ref. [143]. Copyright 2011 Elsevier.

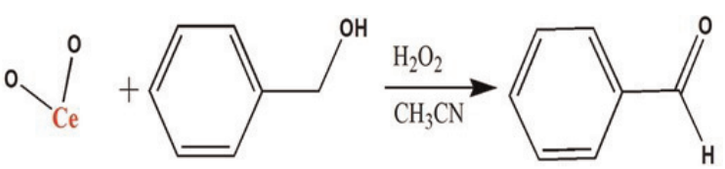

Scheme 1.
Selective oxidation of benzyl alcohol to benzaldehyde. Reprinted with permission from Ref. [142]. Copyright 2017 Scientific Reports.

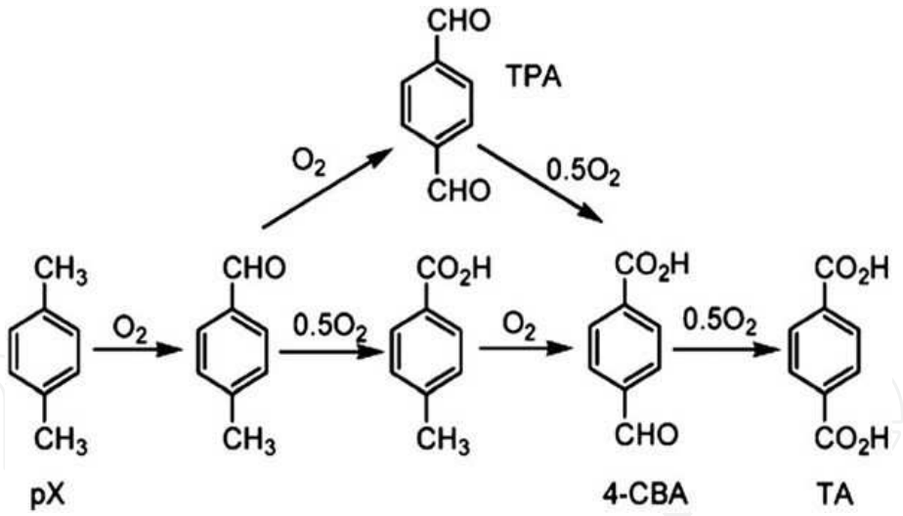

Scheme 2.
Oxidation process for para-xylene to terephthalic acid. Reprinted with permission from Ref. [152]. Copyright 2017 Royal Society of Chemistry.

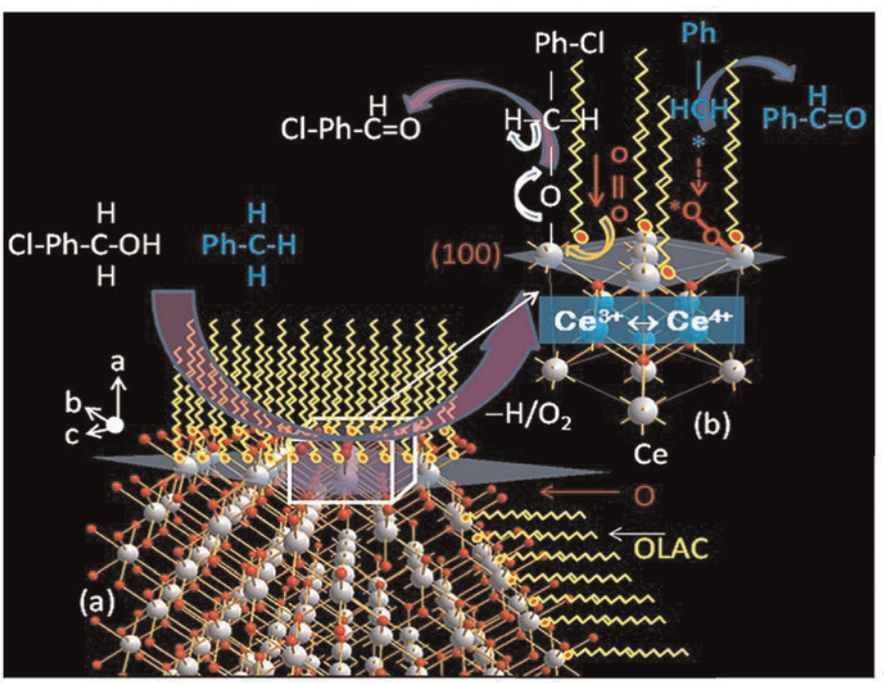

Scheme 3.
Representation of oxidation process of para-chlorobenzyl alcohol/toluene to benzaldehyde by ceria nanocubes. Reprinted with permission from Ref. [153]. Copyright 2017 Royal Society of Chemistry.

stabilizing hydroxyl intermediates is favored over low-vacancy surfaces whereas reverse effect applied for hydrogenation reactions, where nanoparticles are more active than nanocubes [156, 157]. Hydrogen activation on CeO_2 is often regarded as the limiting step of the reaction, even for other functional groups which includes substituted nitroarenes [28, 158]. As already discussed, partial hydrogenation over CeO_2, they have also been employed for the hydrogenation of olefins and carbonyl bonds. For example, a good yield of 1-butene can be obtained by reduction of 1,3-butadiene by Pd/CeO_2 catalyst supported on alumina [159]. Ceria nanostructures evidencing their value in other more complex organic reactions, apart from oxidations and hydrogenations, in advanced and controlled fabrication, promoting it as attractive and versatile nanocatalyst. Coupling reactions including aldol

condensation (**Scheme 4**) [160, 161], Mannich reaction (**Scheme 5**) [162], Suzuki-Miyaura [163], Knoevenagel condensation (**Scheme 6**) [164] or Sonogashira cross couplings [165] have also been reported.

Yadav et al. [166, 167] have cast-off CeO_2 in synthesis. Recent Literature exposed that very few reagents have been reported for the bis-Michael addition reactions and most of the reagents, yielded the mono-Michael addition product [168]. Javad Safaei-Ghomi progressively synthesize CeO_2 nanoparticles and further utilize them by pseudo five-component reaction of acetylenedicarboxylates, phenylhydrazine and aromatic aldehydes in preparation of C-tethered bispyrazol-5-ols at 70°C in water [169]. In organic conversions, as carbon-carbon (C–C) bond formation reactions, the catalytic activity of free-CeO_2 NPs has not been studied extensively to the unsurpassed of our knowledge.

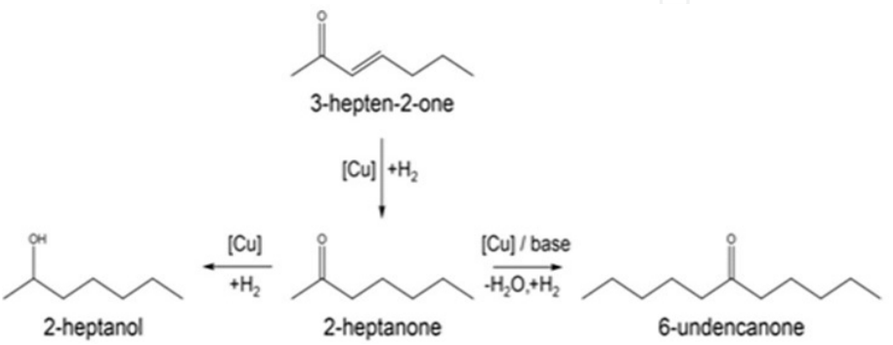

Scheme 4.
Cu supported catalysts on ceria-zirconia catalyzing cross-aldol condensation of acetone and n-butanol into aliphatic ketones. Reprinted with permission from Ref. [160]. Copyright 2017 Catalysts.

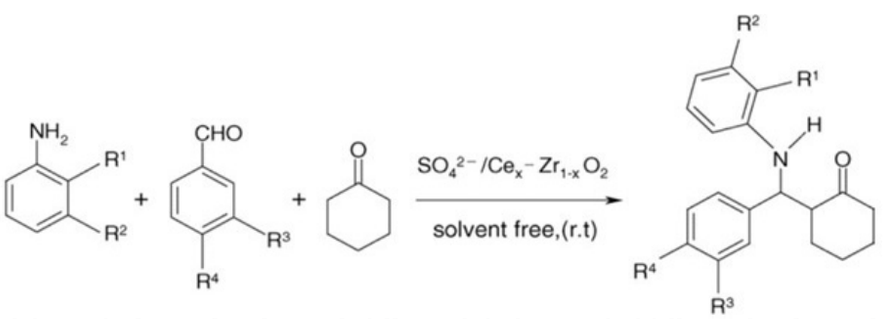

Scheme 5.
Mannich reaction catalyzed by Sulfated $Ce_xZr_{1-x}O_2$ catalyst. Reprinted with permission from Ref. [162]. Copyright 2006 Elsevier.

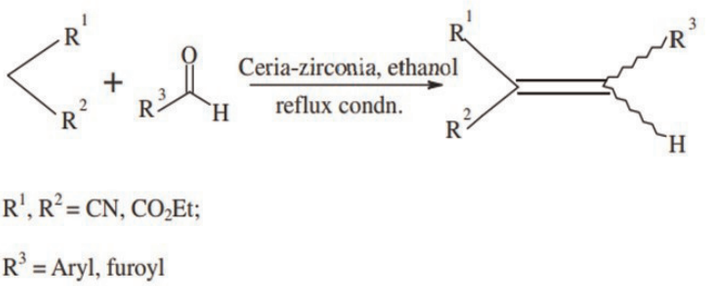

Scheme 6.
Possible mechanism of Knoevenagel condensation. Reprinted with permission from Ref. [164]. Copyright 2009 Elsevier.

3. Conclusion

Various synthetic strategies of Cerium oxide nanoparticles and their progress in the field of catalysis of organic transformations are selectively highlighted in this comprehensive chapter. We presented that at nano level, ceria structures are manipulated with different techniques which allows direct control over catalytic behavior in various reactions. Cerium oxide occupies widespread attention in research on new catalysts with improved properties for organic synthesis due to its very rich chemistry.

Ceria, firstly used by Ford Motor Company as an oxygen storage component, further stepping towards growth in its applications, as consider an "inert" support can stabilize metal nanoparticles which are actively practiced for its catalytic activities, that directly takes part in the reaction with lattice oxygen, afterwards a cocatalyst, and more recently a catalyst. Applications of Ce and Ce-based nanoparticles in different forms of catalysis with recent advances in their preparation methods are properly introduced in the chapter. The synthesis section included different preparation procedures such as hydrothermal, reverse micelle, Co-precipitation and sol-gel method for synthesis of Ce and Ce-based NPs and their characterization. These procedures show their importance in designing and development of Ce-based nanostructures by controlling the morphology of these nanosystems with featured catalytic applications ranging from organic transformations to photocatalysis, and so on. The catalytic improvements of ceria-based nanostructures followed two major directions. First, the surface area is increased with the enhancement of its thermal stability. Second, the nanostructures with well controlled shape and size are obtained by the advent of nanotechnology. While ceria-based materials effectively promoted several oxidation reactions as well as other emerging applications are also proposed.

In addition to this enormous applications of Ce nanocatalysts are reported for organic conversions such as hydrogenation, reduction, alkyne-azide cycloaddition, coupling reactions including A3, coupling. CeO_2 has a good feature as follows: their redox ability and the acid base properties whether they are doped with transition metals or alone. The activation of complex organic molecules with further possible transformation can possibly proceed due to these parameters. Certain acid-base and redox properties can adjust with various cerium-based mixed oxides and to control the number of active sites and their strength for the specific reaction. Latest advances in ceria nanocrystals synthesis with controlled morphologies such as nanocubes, nanorods, polyhedras, etc. should be leading towards encounter of novel catalysts with better selectivities and higher activities in catalysis and organic chemistry.

Acknowledgements

TA thanks to CSIR (Grant No. 01(2897)/17/EMR-II) and SERB-DST (Grant No. EMR/2016/001668), New Delhi, Govt. of India for financial support to research projects. FN and UF are thankful to UGC, New Delhi for Non-NET Research Fellowship.

Conflict of interest

The authors have no conflict of interest.

DOI: http://dx.doi.org/10.5772/intechopen.82688

Author details

Farha Naaz, Umar Farooq and Tokeer Ahmad*
Department of Chemistry, Jamia Millia Islamia, New Delhi, India

*Address all correspondence to: tahmad3@jmi.ac.in

References

[1] Cole-Hamilton DJ. Homogeneous catalysis—New approaches to catalyst separation, recovery, and recycling. Science. 2003;**299**(5613):1702-1706. DOI: 10.1126/science.1081881

[2] Somorjai GA, Li Y. Selective nanocatalysis of organic transformation by metals: Concepts, model systems, and instruments. Topics in Catalysis. 2010;**53**(13–14):832-847. DOI: 10.1007/s11244-010-9511-y

[3] Thomas JM. Colloidal metals: Past, present and future. Pure and Applied Chemistry. 1988;**60**(10):1517-1528. DOI: 10.1351/pac198860101517

[4] Philippot K, Serp P. Concepts in nanocatalysis. In: Nanomater. Catal. 1st ed. New York: John-Wiley & Sons, Inc.; 2012. pp. 1-54. DOI: 10.1002/9783527656875.ch1

[5] Freund PL, Spiro M. Colloidal catalysis: The effect of sol size and concentration. The Journal of Physical Chemistry. 1985;**89**(7):1074-1077. DOI: 10.1021/j100253a007

[6] Babu SG, Karvembu R. Copper based nanoparticles-catalyzed organic transformations. Catalysis Surveys from Asia. 2013;**17**(3–4):156-176. DOI: 10.1007/s10563-013-9159-2

[7] Gladysz JA. Recoverable catalysts. Ultimate goals, criteria of evaluation, and the green chemistry interface. Pure and Applied Chemistry. 2001;**73**(8):1319-1324. DOI: 10.1351/pac200173081319

[8] Gladysz JA. Introduction: Recoverable catalysts and reagents perspective and prospective. Chemical Reviews. 2002;**102**(10):3215-3216. DOI: 10.1021/cr020068s

[9] Suramwar NV, Thakare SR, Khaty NT. Application of Nanomaterials as a Catalyst in Organic Synthesis. International Journal of Knowledge Engineering. 2012;**3**(1):98-99. DOI: 10.9735/0976-5816. ISSN 0976-5816

[10] Ahrens TJ. Global Earth Physic: A Handbook of Physical Constants. Washington, DC: American Geophysical Union; 1995. DOI: 10.14510/araproc.v0i0.1271

[11] Rao H, Jin Y, Fu H, Jiang Y, Zhao Y. A versatile and efficient ligand for copper-catalyzed formation of C**–** N, C**–**O, and P**–**C bonds: Pyrrolidine-2-phosphonic acid phenyl monoester. Chemistry–A European Journal. 2006;**12**(13):3636-3646. DOI: 10.1002/chem.200501473

[12] Kwong FY, Klapars A, Buchwald SL. Copper-catalyzed coupling of alkylamines and aryl iodides: An efficient system even in an air atmosphere. Organic Letters. 2002;**4**(4):581-584. DOI: 10.1021/ol0171867

[13] Kwong FY, Buchwald SL. Mild and efficient copper-catalyzed amination of aryl bromides with primary alkylamines. Organic Letters. 2003;**5**(6):793-796. DOI: 10.1021/ol0273396

[14] Wu TS, Zhou Y, Sabirianov RF, Mei WN, Soo YL, Cheung CL. X-ray absorption study of ceria nanorods promoting the disproportionation of hydrogen peroxide. Chemical Communications. 2016;**52**(28):5003-5006. DOI: 10.1039/C5CC10643E

[15] Celardo I, Pedersen JZ, Traversa E, Ghibelli L. Pharmacological potential of cerium oxide nanoparticles. Nanoscale. 2011;**3**(4):1411-1420. DOI: 10.1039/C0NR00875C

[16] Esch F, Fabris S, Zhou L, Montini T, Africh C, Fornasiero P, et al. Electron localization determines defect

formation on ceria substrates. Science. 2005;**309**(5735):752-755. DOI: 10.1126/science.1111568

[17] Lawrence NJ, Brewer JR, Wang L, Wu TS, Wells-Kingsbury J, Ihrig MM, et al. Defect engineering in cubic cerium oxide nanostructures for catalytic oxidation. Nano Letters. 2011;**11**(7):2666-2671. DOI: 10.1021/nl200722z

[18] Liu W, Wang W, Tang K, Guo J, Ren Y, Wang S, et al. The promoting influence of nickel species in the controllable synthesis and catalytic properties of nickel–ceria catalysts. Catalysis Science & Technology. 2016;**6**(7):2427-2434. DOI: 10.1039/C5CY01241D

[19] Lu G, Linsebigler A, Yates JT Jr. Photooxidation of CH_3Cl on TiO_2 (110): A mechanism not involving H_2O. The Journal of Physical Chemistry. 1995;**99**(19):7626-7631. DOI: 10.1021/j100019a049

[20] Bai S, Shi B, Deng W, Dai Q, Wang X. Catalytic oxidation of 1, 2-dichloroethane over Al_2O_3–CeO_2 catalysts: Combined effects of acid and redox properties. RSC Advances. 2015;**5**(60):48916-48927. DOI: 10.1039/C5RA07405C

[21] Yuan Q, Duan HH, Li LL, Sun LD, Zhang YW, Yan CH. Controlled synthesis and assembly of ceria-based nanomaterials. Journal of Colloid and Interface Science. 2009;**335**(2):151-167. DOI: 10.1016/j.jcis.2009.04.007

[22] Huang W, Gao Y. Morphology-dependent surface chemistry and catalysis of CeO_2 nanocrystals. Catalysis Science & Technology. 2014;**4**(11):3772-3784. DOI: 10.1039/C4CY00679H

[23] Montini T, Melchionna M, Monai M, Fornasiero P. Fundamentals and catalytic applications of CeO_2-based materials. Chemical Reviews. 2016;**116**(10):5987-6041. DOI: 10.1021/acs.chemrev.5b00603

[24] Paier J, Penschke C, Sauer J. Oxygen defects and surface chemistry of ceria: Quantum chemical studies compared to experiment. Chemical Reviews. 2013;**113**(6):3949-3985. DOI: 10.1021/cr3004949

[25] Fan L, Wang C, Chen M, Zhu B. Recent development of ceria-based (nano) composite materials for low temperature ceramic fuel cells and electrolyte-free fuel cells. Journal of Power Sources. 2013;**234**:154-174. DOI: 10.1016/j.jpowsour.2013.01.138

[26] Sun C, Li H, Chen L. Nanostructured ceria-based materials: Synthesis, properties, and applications. Energy & Environmental Science. 2012;**5**(9):8475-8505. DOI: 10.1039/C2EE22310D

[27] Mogensen M, Sammes NM, Tompsett GA. Physical, chemical and electrochemical properties of pure and doped ceria. Solid State Ionics. 2000;**129**(1–4):63-94. DOI: 10.1016/S0167-2738(99)00318-5

[28] Vivier L, Duprez D. Ceria-based solid catalysts for organic chemistry. ChemSusChem. 2010;**3**(6):654-678. DOI: 10.1002/cssc.201000054

[29] Zhang D, Du X, Shi L, Gao R. Shape-controlled synthesis and catalytic application of ceria nanomaterials. Dalton Transactions. 2012;**41**(48):14455-14475. DOI: 10.1039/C2DT31759A

[30] Trovarelli A. Catalytic properties of ceria and CeO_2-containing materials. Catalysis Reviews. 1996;**38**(4):439-520. DOI: 10.1080/01614949608006464

[31] Mandoli C, Pagliari F, Pagliari S, Forte G, Di Nardo P, Licoccia S, et al. Stem cell aligned growth induced by CeO_2 nanoparticles in PLGA scaffolds

with improved bioactivity for regenerative medicine. Advanced Functional Materials. 2010;**20**(10): 1617-1624. DOI: 10.1002/adfm.200902363

[32] Xu C, Lin Y, Wang J, Wu L, Wei W, Ren J, et al. Nanoceria-triggered synergetic drug release based on CeO_2-capped mesoporous silica host–guest interactions and switchable enzymatic activity and cellular effects of CeO_2. Advanced Healthcare Materials. 2013; **2**(12):1591-1599. DOI: 10.1002/adhm.201200464

[33] Kim CK, Kim T, Choi IY, Soh M, Kim D, Kim YJ, et al. Ceria nanoparticles that can protect against ischemic stroke. Angewandte Chemie International Edition. 2012;**51**(44): 11039-11043. DOI: 10.1002/anie.201203780

[34] Furler P, Scheffe JR, Steinfeld A. Syngas production by simultaneous splitting of H_2O and CO_2 via ceria redox reactions in a high-temperature solar reactor. Energy & Environmental Science. 2012;**5**(3):6098-6103. DOI: 10.1039/C1EE02620H

[35] Scheffe JR, Welte M, Steinfeld A. Thermal reduction of ceria within an aerosol reactor for H_2O and CO_2 splitting. Industrial & Engineering Chemistry Research. 2014;**53**(6): 2175-2182. DOI: 10.1021/ie402620k

[36] Vyas S. Simulation of ceria: Bulk and surface defects [doctoral dissertation]. University of London; 1997

[37] Fronzi M, Soon A, Delley B, Traversa E, Stampfl C. Stability and morphology of cerium oxide surfaces in an oxidizing environment: A first-principles investigation. The Journal of Chemical Physics. 2009;**131**(10):104701. DOI: 10.1063/1.3191784

[38] Sayle TXT, Parker SC, Catlow CRA. The role of oxygen vacancies on ceria surfaces in the oxidation of carbon monoxide. Surface Science. 1994; **316**(3):329-336. DOI: 10.1016/0039-6028(94)91225-4

[39] Kaneko K, Inoke K, Freitag B, Hungria AB, Midgley PA, Hansen TW, et al. Structural and morphological characterization of cerium oxide nanocrystals prepared by hydrothermal synthesis. Nano Letters. 2007;**7**(2): 421-425. DOI: 10.1021/nl062677b

[40] Otsuka-Yao-Matsuo S, Omata T, Izu N, Kishimoto H. Oxygen release behavior of $CeZrO_4$ powders and appearance of new compounds k and t. Journal of Solid State Chemistry. 1998; **138**(1):47-54. DOI: 10.1006/jssc.1998.7753

[41] Mai HX, Sun LD, Zhang YW, Si R, Feng W, Zhang HP, et al. Shape-selective synthesis and oxygen storage behavior of ceria nanopolyhedra, nanorods, and nanocubes. The Journal of Physical Chemistry B. 2005;**109**(51): 24380-24385. DOI: 10.1021/jp055584b

[42] Trovarelli A, Llorca J. Ceria catalysts at nanoscale: How do crystal shapes shape catalysis? ACS Catalysis. 2017; **7**(7):4716-4735. DOI: 10.1021/acscatal.7b01246

[43] Singh SB, Tandon PK. Catalysis: A brief review on nano-catalyst. Journal of Energy and Chemical Engineering. 2014;**2**(3):106-115. DOI: 10.4172/2157-7439-C1-058

[44] Chen L, Fleming P, Morris V, Holmes JD, Morris MA. Size-related lattice parameter changes and surface defects in ceria nanocrystals. The Journal of Physical Chemistry C. 2010; **114**(30):12909-12919. DOI: 10.1021/jp1031465

[45] Hua G, Zhang L, Fei G, Fang M. Enhanced catalytic activity induced by defects in mesoporous ceria nanotubes. Journal of Materials Chemistry. 2012;

22(14):6851-6855. DOI: DOI :10.1039/c2jm13610d

[46] Tang CC, Bando Y, Liu BD, Golberg D. Cerium oxide nanotubes prepared from cerium hydroxide nanotubes. Advanced Materials. 2005;**17**(24): 3005-3009. DOI: 10.1002/adma.200501557

[47] Averill BA. Principles of General Chemistry2012. pp. 1403-1521

[48] Stratton TG, Tuller HL. Thermodynamic and transport studies of mixed oxides. The CeO_2–UO_2 system. Journal of the Chemical Society, Faraday Transactions 2: Molecular and Chemical Physics. 1987;**83**(7):1143-1156. DOI: 10.1039/F29878301143

[49] Tuller HL, Bishop SR. Tailoring material properties through defect engineering. Chemistry Letters. 2010; **39**(12):1226-1231. DOI: 10.1246/cl.2010.1226

[50] Li J, Zhang Z, Tian Z, Zhou X, Zheng Z, Ma Y, et al. Low pressure induced porous nanorods of ceria with high reducibility and large oxygen storage capacity: Synthesis and catalytic applications. Journal of Materials Chemistry A. 2014;**2**(39):16459-16466. DOI: 10.1039/C4TA03718A

[51] Bernal S, Calvino JJ, Cauqui MA, Gatica JM, Larese C, Omil JP, et al. Some recent results on metal/support interaction effects in NM/CeO_2 (NM: noble metal) catalysts. Catalysis Today. 1999;**50**(2):175-206. DOI: 10.1016/S0920-5861(98)00503-3

[52] Nilsson A, Pettersson LGM. Chemical bonding on surfaces probed by X-ray emission spectroscopy and density functional theory. Surface Science Reports. 2004;**55**(2–5):49-167. DOI: 10.1016/j.surfrep.2004.06.002

[53] Lawrence NJ. Synthesis and catalytic activity of nanostructured cerium oxide [dissertation]. 2010

[54] Aneggi E, Boaro M, de Leitenburg C, Dolcetti G, Trovarelli A. Insights into the redox properties of ceria-based oxides and their implications in catalysis. Journal of Alloys and Compounds. 2006;**408**:1096-1102. DOI: 10.1016/j.jallcom.2004.12.113

[55] Wang G, Wang L, Fei X, Zhou Y, Sabirianov RF, Mei WN, et al. Probing the bifunctional catalytic activity of ceria nanorods towards the cyanosilylation reaction. Catalysis Science & Technology. 2013;**3**(10): 2602-2609. DOI: 10.1039/C3CY00196B

[56] Khaladji J, Peltier M, Rhone-Poulenc Industries. Rare earth polishing compositions. U.S. Patent 4,942,697; 1990

[57] Liu L, Yao Z, Deng Y, Gao F, Liu B, Dong L. Morphology and crystal-plane effects of nanoscale ceria on the activity of CuO/CeO_2 for NO reduction by CO. ChemCatChem. 2011;**3**(6):978-989. DOI: 10.1002/cctc.201000320

[58] Sabot J-L, Maestro P. Kirk-Othmer Encyclopedia of Chemical Technology. New York: John Wiley & Sons, Inc.; 2000. DOI: 10.1007/978-90-481-8679-2

[59] Schermanz K, Sagar A, TreibacherIndustrie AG. Ceria zirconia alumina composition with enhanced thermal stability. U.S. Patent 9,475,035; 2016

[60] Wang JF, Rohm and Haas Electronic Materials CMP Inc. Oxide particles and method for producing them. U.S. Patent 5,389,352; 1995

[61] Hanawa K, Mochizuki N, Ueda N, Mitsui Mining and Smelting Co Ltd. Cerium oxide ultrafine particles and method for preparing the same. U.S. Patent 5,938,837; 1999

[62] Rogal J, Reuter K, Scheffler M. CO oxidation at Pd (100): A first-principles constrained thermodynamics study.

Physical Review B. 2007;**75**(20):205433. DOI: 10.1103/PhysRevB.75.205433

[63] Mavrikakis M, Hammer B, Nørskov JK. Effect of strain on the reactivity of metal surfaces. Physical Review Letters. 1998;**81**(13):2819. DOI: DOI : 10.1103/PhysRevLett.81.2819

[64] Grabow L, Xu Y, Mavrikakis M. Lattice strain effects on CO oxidation on Pt (111). Physical Chemistry Chemical Physics. 2006;**8**(29):3369-3374. DOI: 10.1039/B606131A

[65] Greeley J, Krekelberg WP, Mavrikakis M. Strain-induced formation of subsurface species in transition metals. Angewandte Chemie. 2004; **116**(33):4396-4400. DOI: 10.1002/ange.200454062

[66] Venezia AM, Pantaleo G, Longo A, Di Carlo G, Casaletto MP, Liotta FL, et al. Relationship between structure and CO oxidation activity of ceria-supported gold catalysts. The Journal of Physical Chemistry B. 2005;**109**(7): 2821-2827. DOI: 10.1021/jp045928i

[67] Senanayake SD, Stacchiola D, Rodriguez JA. Unique properties of ceria nanoparticles supported on metals: Novel inverse ceria/copper catalysts for CO oxidation and the water-gas shift reaction. Accounts of Chemical Research. 2013;**46**(8):1702-1711. DOI: 10.1021/ar300231p

[68] Wang F. Structural and electronic properties of noble metals on metal oxide surfaces [doctoral dissertation]. 2011

[69] White RJ, Luque R, Budarin VL, Clark JH, Macquarrie DJ. Supported metal nanoparticles on porous materials. Methods and applications. Chemical Society Reviews. 2009;**38**(2):481-494. DOI: 10.1039/B802654H

[70] Vantomme A, Yuan ZY, Du G, Su BL. Surfactant-assisted large-scale preparation of crystalline CeO_2 nanorods. Langmuir. 2005;**21**(3): 1132-1135. DOI: 10.1021/la047751p

[71] Lu X, Zhai T, Cui H, Shi J, Xie S, Huang Y, et al. Redox cycles promoting photocatalytic hydrogen evolution of CeO_2 nanorods. Journal of Materials Chemistry. 2011;**21**(15):5569-5572. DOI: 10.1039/C0JM04466K

[72] Sun C, Sun J, Xiao G, Zhang H, Qiu X, Li H, et al. Mesoscale organization of nearly monodisperse flowerlike ceria microspheres. The Journal of Physical Chemistry B. 2006;**110**(27): 13445-13452. DOI: 10.1021/jp062179r

[73] Xie X, Li Y, Liu ZQ, Haruta M, Shen W. Low-temperature oxidation of CO catalysed by Co_3O_4 nanorods. Nature. 2009;**458**(7239):746. DOI: 10.1038/nature07877

[74] Yang HG, Sun CH, Qiao SZ, Zou J, Liu G, Smith SC, et al. Anatase TiO_2 single crystals with a large percentage of reactive facets. Nature. 2008;**453**(7195): 638. DOI: 10.1038/nature06964

[75] Leng M, Liu M, Zhang Y, Wang Z, Yu C, Yang X, et al. Polyhedral 50-facet Cu_2O microcrystals partially enclosed by {311} high-index planes: Synthesis and enhanced catalytic CO oxidation activity. Journal of the American Chemical Society. 2010;**132**(48): 17084-17087. DOI: 10.1021/ja106788x

[76] Wang ZL, Feng X. Polyhedral shapes of CeO_2 nanoparticles. The Journal of Physical Chemistry B. 2003; **107**(49):13563-13566. DOI: 10.1021/jp036815m

[77] Hirano M, Fukuda Y, Iwata H, Hotta Y, Inagaki M. Preparation and spherical agglomeration of crystalline cerium (IV) oxide nanoparticles by thermal hydrolysis. Journal of the American Ceramic Society. 2000;**83**(5):1287-1289. DOI: 10.1111/j.1151-2916. 2000.tb01371.x

[78] Zhou F, Zhao X, Xu H, Yuan C. CeO_2 spherical crystallites: Synthesis, formation mechanism, size control, and electrochemical property study. The Journal of Physical Chemistry C. 2007; **111**(4):1651-1657. DOI: 10.1021/jp0660435

[79] Xia B, Lenggoro IW, Okuyama K. Synthesis of CeO_2 nanoparticles by salt-assisted ultrasonic aerosol decomposition. Journal of Materials Chemistry. 2001;**11**(12):2925-2927. DOI: 10.1039/B105548H

[80] Wang S, Zhao L, Wang W, Zhao Y, Zhang G, Ma X, et al. Morphology control of ceria nanocrystals for catalytic conversion of CO_2 with methanol. Nanoscale. 2013;**5**(12): 5582-5588. DOI: 10.1039/C3NR00831B

[81] Dai Q, Bai S, Li H, Liu W, Wang X, Lu G. Template-free and non-hydrothermal synthesis of CeO_2 nanosheets via a facile aqueous-phase precipitation route with catalytic oxidation properties. CrystEngComm. 2014;**16**(42):9817-9827. DOI: 10.1039/C4CE01436G

[82] Zhou K, Wang X, Sun X, Peng Q, Li Y. Enhanced catalytic activity of ceria nanorods from well-defined reactive crystal planes. Journal of Catalysis. 2005;**229**(1):206-212. DOI: 10.1016/j.jcat.2004.11.004

[83] Dai Q, Huang H, Zhu Y, Deng W, Bai S, Wang X, et al. Catalysis oxidation of 1, 2-dichloroethane and ethyl acetate over ceria nanocrystals with well-defined crystal planes. Applied Catalysis B: Environmental. 2012;**117**:360-368. DOI: 10.1016/j.apcatb.2012.02.001

[84] Choi M, Na K, Kim J, Sakamoto Y, Terasaki O, Ryoo R. Stable single-unit-cell nanosheets of zeolite MFI as active and long-lived catalysts. Nature. 2009; **461**(7261):246. DOI: 10.1038/nature08288

[85] Kim JE, Carroll PJ, Schelter EJ. Bidentate nitroxide ligands stable toward oxidative redox cycling and their complexes with cerium and lanthanum. Chemical Communications. 2015; **51**(81):15047-15050. DOI: 10.1039/C5CC06052D

[86] Qi J, Chen J, Li G, Li S, Gao Y, Tang Z. Facile synthesis of core–shell Au@CeO_2 nanocomposites with remarkably enhanced catalytic activity for CO oxidation. Energy & Environmental Science. 2012;**5**(10):8937-8941. DOI: 10.1039/C2EE22600F

[87] Mitsudome T, Mikami Y, Matoba M, Mizugaki T, Jitsukawa K, Kaneda K. Design of a silver–cerium dioxide core–shell nanocomposite catalyst for chemoselective reduction reactions. Angewandte Chemie International Edition. 2012;**51**(1):136-139

[88] Saada R, Kellici S, Heil T, Morgan D, Saha B. Greener synthesis of dimethyl carbonate using a novel ceria–zirconia oxide/graphene nanocomposite catalyst. Applied Catalysis B: Environmental. 2015;**168**:353-362. DOI: 10.1016/j.apcatb.2014.12.013

[89] Cargnello M, Wieder NL, Montini T, Gorte RJ, Fornasiero P. Synthesis of dispersible Pd@CeO_2 core-shell nanostructures by self-assembly. Journal of the American Chemical Society. 2009;**132**(4):1402-1409. DOI: 10.1021/ja909131k

[90] Yamada Y, Tsung CK, Huang W, Huo Z, Habas SE, Soejima T, et al. Nanocrystal bilayer for tandem catalysis. Nature Chemistry. 2011;**3**(5): 372. DOI: 10.1038/nchem.1018

[91] Grinter DC, Ithnin R, Pang CL, Thornton G. Defect structure of ultrathin ceria films on Pt (111): Atomic views from scanning tunnelling microscopy. The Journal of Physical Chemistry C. 2010;**114**(40): 17036-17041. DOI: 10.1021/jp102895k

[92] Rodriguez JA, Grinter DC, Liu Z, Palomino RM, Senanayake SD. Ceria-based model catalysts: Fundamental studies on the importance of the metal–ceria interface in CO oxidation, the water-gas shift, CO_2 hydrogenation, and methane and alcohol reforming. Chemical Society Reviews. 2017;**46**(7): 1824-1841. DOI: 10.1039/C6CS00863A

[93] Harding C, Habibpour V, Kunz S, Farnbacher ANS, Heiz U, Yoon B, et al. Control and manipulation of gold nanocatalysis: Effects of metal oxide support thickness and composition. Journal of the American Chemical Society. 2008;**131**(2):538-548. DOI: 10.1021/ja804893b

[94] Campbell CT, Parker SC, Starr DE. The effect of size-dependent nanoparticle energetics on catalyst sintering. Science. 2002;**298**(5594): 811-814. DOI: 10.1126/science.1075094

[95] Renaud G, Lazzari R, Revenant C, Barbier A, Noblet M, Ulrich O, et al. Real-time monitoring of growing nanoparticles. Science. 2003;**300**(5624): 1416-1419. DOI: 10.1126/science.1082146

[96] Conner WC Jr, Falconer JL. Spillover in heterogeneous catalysis. Chemical Reviews. 1995;**95**(3):759-788. DOI: 10.1021/cr00035a014

[97] Libuda J, Freund HJ. Molecular beam experiments on model catalysts. Surface Science Reports. 2005;**57**(7–8): 157-298. DOI: 10.1016/j.surfrep.2005.03.002

[98] Vayssilov GN, Lykhach Y, Migani A, Staudt T, Petrova GP, Tsud N, et al. Support nanostructure boosts oxygen transfer to catalytically active platinum nanoparticles. Nature Materials. 2011; **10**(4):310. DOI: 10.1038/nmat2976

[99] Bond GC, Thompson DT. Catalysis by gold. Catalysis Reviews. 1999;**41**(3–4): 319-388. DOI: 10.1081/CR-100101171

[100] Bunluesin T, Gorte RJ, Graham GW. CO oxidation for the characterization of reducibility in oxygen storage components of three-way automotive catalysts. Applied Catalysis B: Environmental. 1997;**14** (1–2):105-115. DOI: 10.1016/S0926-3373(97)00016-7

[101] Putna ES, Bunluesin T, Fan XL, Gorte RJ, Vohs JM, Lakis RE, et al. Ceria films on zirconia substrates: Models for understanding oxygen-storage properties. Catalysis Today. 1999;**50**(2): 343-352. DOI: 10.1016/S0920-5861(98)00514-8

[102] Cordatos H, Bunluesin T, Stubenrauch J, Vohs JM, Gorte RJ. Effect of ceria structure on oxygen migration for Rh/ceria catalysts. The Journal of Physical Chemistry. 1996; **100**(2):785-789. DOI: 10.1021/jp952050+

[103] Mamontov E, Egami T, Brezny R, Koranne M, Tyagi S. Lattice defects and oxygen storage capacity of nanocrystalline ceria and ceria-zirconia. The Journal of Physical Chemistry B. 2000;**104**(47):11110-11116. DOI: 10.1021/jp0023011

[104] Fornasiero P, Dimonte R, Rao GR, Kaspar J, Meriani S, Trovarelli AO, et al. Rh-loaded CeO_2-ZrO_2 solid-solutions as highly efficient oxygen exchangers: Dependence of the reduction behavior and the oxygen storage capacity on the structural-properties. Journal of Catalysis. 1995;**151**(1):168-177. DOI: 10.1006/jcat.1995.1019

[105] Fornasiero P, Balducci G, Di Monte R, Kašpar J, Sergo V, Gubitosa G, et al. Modification of the redox behaviour of CeO_2 induced by structural doping with ZrO_2. Journal of Catalysis. 1996; **164**(1):173-183. DOI: 10.1006/jcat.1996.0373

[106] Vidmar P, Fornasiero P, Kaspar J, Gubitosa G, Graziani M, Catal J. Effects of trivalent dopants on the redox

properties of $Ce_{0.6}Zr_{0.4}O_2$ mixed oxide. Journal of Catalysis. 1997;**171**(1): 160-168. DOI: 10.1006/jcat.1987.1784

[107] Fornasiero P, Kašpar J, Sergo V, Graziani M. Redox behavior of high-surface-area Rh-, Pt-, and Pd-loaded $Ce_{0.5}Zr_{0.5}O_2$ mixed oxide. Journal of Catalysis. 1999;**182**(1):56-69. DOI: 10.1006/jcat.1998.2321

[108] Vlaic G, Fornasiero P, Geremia S, Kašpar J, Graziani M. Relationship between the zirconia-promoted reduction in the Rh-loaded $Ce_{0.5}Zr_{0.5}O_2$ mixed oxide and the Zr–O local structure. Journal of Catalysis. 1997; **168**(2):386-392. DOI: 10.1006/ jcat.1997.1644

[109] Vlaic G, Di Monte R, Fornasiero P, Fonda E, Kašpar J, Graziani M. Redox property–local structure relationships in the Rh-loaded CeO_2–ZrO_2 mixed oxides. Journal of Catalysis. 1999;**182**(2): 378-389. DOI: 10.1006/jcat.1998.2335

[110] Fornasiero P, Fonda E, Di Monte R, Vlaic G, Kašpar J, Graziani M. Relationships between structural/ textural properties and redox behavior in $Ce_{0.6}Zr_{0.4}O_2$ mixed oxides. Journal of Catalysis. 1999;**187**(1):177-185. DOI: 10.1006/jcat.1999.2589

[111] Rodriguez JA, Liu P, Graciani J, Senanayake SD, Grinter DC, Stacchiola D, et al. Inverse oxide/metal catalysts in fundamental studies and practical applications: A perspective of recent developments. The Journal of Physical Chemistry Letters. 2016;7(13): 2627-2639. DOI: 10.1021/acs. jpclett.6b00499

[112] Rodriguez JA, Liu P, Graciani J, Senanayake SD, Grinter DC, Stacchiola D, et al. Inverse oxide/metal catalysts in fundamental studies and practical applications: A perspective of recent developments. The Journal of Physical Chemistry Letters. 2016;7(13):2627-2639. DOI: 10.1021/acs.jpclett.6b00499

[113] Raimondi F, Scherer GG, Kötz R, Wokaun A. Nanoparticles in energy technology: Examples from electrochemistry and catalysis. Angewandte Chemie International Edition. 2005;**44**(15):2190-2209. DOI: 10.1002/anie.200460466

[114] Vayssilov GN, Migani A, Neyman K. Density functional modeling of the interactions of platinum clusters with CeO_2 nanoparticles of different size. The Journal of Physical Chemistry C. 2011; **115**(32):16081-16086. DOI: 10.1021/ jp204222k

[115] Wang JH, Liu M, Lin MC. Oxygen reduction reactions in the SOFC cathode of Ag/CeO_2. Solid State Ionics. 2006;**177** (9–10):939-947. DOI: 10.1016/j. ssi.2006.02.029

[116] Vári G, Óvári L, Kiss J, Kónya Z. LEIS and XPS investigation into the growth of cerium and cerium dioxide on Cu (111). Physical Chemistry Chemical Physics. 2015;**17**(7):5124-5132. DOI: 10.1039/C4CP05179C

[117] Zhou Y. Nanostructured cerium oxide-based catalysts: Synthesis, physical properties, and catalytic performance [doctoral dissertation]. 2015

[118] Eyring L. The binary lanthanide oxides: Synthesis and identification. In: Synthesis of Lanthanide and Actinide Compounds. Dordrecht: Springer; 1991. pp. 187-224. DOI: 10.1007/978-94-011-3758-4-8

[119] De Leitenburg C, Trovarelli A, Kašpar J. A temperature-programmed and transient kinetic study of CO_2 activation and methanation over CeO_2 supported noble metals. Journal of Catalysis. 1997;**166**(1):98-107. DOI: 10.1006/jcat.1997.1498

[120] Audebrand N, Auffrédic JP, Louër D. An X-ray powder diffraction study of

the microstructure and growth kinetics of nanoscale crystallites obtained from hydrated cerium oxides. Chemistry of Materials. 2000;**12**(6):1791-1799. DOI: 10.1021/cm001013e

[121] Nakane S, Tachi T, Yoshinaka M, Hirota K, Yamaguchi O. Characterization and sintering of reactive cerium (IV) oxide powders prepared by the hydrazine method. Journal of the American Ceramic Society. 1997;**80**(12):3221-3224. DOI: 10.1111/j.1151-2916.1997.tb03255.x

[122] Abimanyu H, Ahn BS, Kim CS, Yoo KS. Preparation and characterization of MgO-CeO_2 mixed oxide catalysts by modified coprecipitation using ionic liquids for dimethyl carbonate synthesis. Industrial & Engineering Chemistry Research. 2007;**46**(24):7936-7941. DOI: 10.1021/ie070528d

[123] Ward DA, Ko EI. Preparing catalytic materials by the sol-gel method. Industrial & Engineering Chemistry Research. 1995;**34**(2): 421-433. DOI: 10.1021/ie00041a001

[124] Gnanam S, Rajendran V. Synthesis of CeO_2 or α-Mn_2O_3 nanoparticles via sol–gel process and their optical properties. Journal of Sol-Gel Science and Technology. 2011;**58**(1):62-69. DOI: 10.1007/s10971-010-2356-9

[125] Masui T, Fujiwara K, Machida KI, Adachi GY, Sakata T, Mori H. Characterization of cerium (IV) oxide ultrafine particles prepared using reversed micelles. Chemistry of Materials. 1997;**9**(10):2197-2204. DOI: 10.1021/cm970359v

[126] Vaidya S, Agarwal S, Ahmad T, Ganguli AK. Nanocrystalline oxalate/carbonate precursors of Ce and Zr and their decompositions to CeO_2 and ZrO_2 nanoparticles. Journal of American Ceramic Society. 2007;**90**(3):863-869. DOI: 10.1111/j.1551-2916.2007.01484.x

[127] Ganguli AK, Vaidya S, Ahmad T. Synthesis of nanocrystalline materials through reverse micelles: A versatile methodology for synthesis of complex metal oxides. Bulletin of Materials Science. 2008;**31**(3):415-419. DOI: 10.1007/s12034-008-0065-6

[128] Ahmad T, Shahazad M, Ubaidullah M, Ahmed J, Khan A, El-Toni AM. Structural characterization and dielectric properties of ceria–titania nanocomposites in low ceria region. Materials Research Express. 2017;**4**(12):125016. DOI: 10.1088/2053-1591/aa9c51

[129] Ahmad T, Shahazad M, Ubaidullah M, Ahmed J. Synthesis, characterization and dielectric properties of TiO_2-CeO_2 ceramic nanocomposites at low titania concentration. Bulletin of Materials Science. 2018;**41**(4):99. DOI: 10.1007/s12034-018-1616-0

[130] Ahmed J, Ahmad T, Ramanujachary KV, Lofland SE, Ganguli AK. Development of a microemulsion-based process for synthesis of cobalt (Co) and cobalt oxide (Co_3O_4) nanoparticles from submicrometer rods of cobalt oxalate. Journal of Colloid and Interface Science. 2008;**321**(2):434-441. DOI: 10.1016/j.jcis.2008.01.052

[131] Ganguly A, Trinh P, Ramanujachary KV, Ahmad T, Mugweru A, Ganguli AK. Reverse micellar based synthesis of ultrafine MgO nanoparticles (8–10 nm): Characterization and catalytic properties. Journal of Colloid and Interface Science. 2011;**353**(1):137-142. DOI: 10.1016/j.jcis.2010.09.041

[132] Lyons DM, McGrath JP, Morris MA. Surface studies of ceria and mesoporous ceria powders by solid-state 1H MAS NMR. The Journal of Physical Chemistry B. 2003;**107**(19):4607-4617. DOI: 10.1021/jp0341570

[133] Terribile D, Trovarelli A, Llorca J, de Leitenburg C, Dolcetti G. The synthesis and characterization of mesoporous high-surface area ceria prepared using a hybrid organic/inorganic route. Journal of Catalysis. 1998;**178**(1):299-308. DOI: 10.1006/jcat.1998.2152

[134] Carreon MA, Guliants VV. Ordered meso-and macroporous binary and mixed metal oxides. European Journal of Inorganic Chemistry. 2005;**2005**(1):27-43. DOI: 10.1002/ejic.200400675

[135] Hojo H, Mizoguchi T, Ohta H, Findlay SD, Shibata N, Yamamoto T, et al. Atomic structure of a CeO_2 grain boundary: The role of oxygen vacancies. Nano Letters. 2010;**10**(11):4668-4672. DOI: 10.1021/nl1029336

[136] Bhatta UM, Ross IM, Sayle TX, Sayle DC, Parker SC, Reid D, et al. Cationic surface reconstructions on cerium oxide nanocrystals: An aberration-corrected HRTEM study. ACS Nano. 2012;**6**(1):421-430. DOI: 10.1021/nn2037576

[137] Haruta M. Nanoparticulate gold catalysts for low-temperature CO oxidation. Journal of New Materials for Electrochemical Systems. 2004;**7**:163-172. DOI: 10.1016/j.apcatb.2003.11.003

[138] Sun C, Li H, Chen L. Study of flowerlike CeO_2 microspheres used as catalyst supports for CO oxidation reaction. Journal of Physics and Chemistry of Solids. 2007;**68**(9):1785-1790. DOI: 10.1016/j.jpcs.2007.05.005

[139] Conesa J. Computer modeling of surfaces and defects on cerium dioxide. Surface Science. 1995;**339**(3):337-352. DOI: 10.1016/0039-6028(95)00595-1

[140] Piumetti M, Andana T, Bensaid S, Russo N, Fino D, Pirone R. Study on the CO oxidation over ceria-based nanocatalysts. Nanoscale Research Letters. 2016;**11**(1):165. DOI: 10.1186/s11671-016-1375-z

[141] Yan L, Yu R, Chen J, Xing X. Template-free hydrothermal synthesis of CeO_2 nano-octahedrons and nanorods: Investigation of the morphology evolution. Crystal Growth and Design. 2008;**8**(5):1474-1477. DOI: 10.1021/cg800117v

[142] Tamizhdurai P, Sakthinathan S, Chen SM, Shanthi K, Sivasanker S, Sangeetha P. Environmentally friendly synthesis of CeO_2 nanoparticles for the catalytic oxidation of benzyl alcohol to benzaldehyde and selective detection of nitrite. Scientific Reports. 2017;**7**:46372. DOI: 10.1038/srep46372

[143] Wu Z, Li M, Overbury SH. On the structure dependence of CO oxidation over CeO_2 nanocrystals with well-defined surface planes. Journal of Catalysis. 2012;**285**(1):61-73. DOI: 10.1016/j.jcat.2011.09.011

[144] Wang X, Jiang Z, Zheng B, Xie Z, Zheng L. Synthesis and shape-dependent catalytic properties of CeO_2 nanocubes and truncated octahedra. CrystEngComm. 2012;**14**(22):7579-7582. DOI: 10.1039/C2CE25333J

[145] Zhou HP, Zhang YW, Si R, Zhang LS, Song WG, Yan CH. Dimension-manipulated ceria nanostructures (0D uniform nanocrystals, 2D polycrystalline assembly, and 3D mesoporous framework) from cerium octylate precursor in solution phases and their CO oxidation activities. The Journal of Physical Chemistry C. 2008;**112**(51):20366-20374. DOI: 10.1021/jp807091n

[146] Li J, Lu G, Li H, Wang Y, Guo Y, Guo Y. Facile synthesis of 3D flowerlike CeO_2 microspheres under mild condition with high catalytic performance for CO oxidation. Journal

of Colloid and Interface Science. 2011; **360**(1):93-99. DOI: 10.1016/j.jcis.2011.04.052

[147] Cui R, Lu W, Zhang L, Yue B, Shen S. Template-free synthesis and self-assembly of CeO_2 nanospheres fabricated with foursquare nanoflakes. The Journal of Physical Chemistry C. 2009;**113**(52):21520-21525. DOI: 10.1021/jp9065168

[148] Renuka NK, Praveen AK, Aniz CU. Ceria rhombic microplates: Synthesis, characterization and catalytic activity. Microporous and Mesoporous Materials. 2013;**169**:35-41. DOI: 10.1016/j.micromeso.2012.10.010

[149] Li J, Zhang Z, Gao W, Zhang S, Ma Y, Qu Y. Pressure regulations on the surface properties of CeO_2 nanorods and their catalytic activity for CO oxidation and nitrile hydrolysis reactions. ACS Applied Materials & Interfaces. 2016; **8**(35):22988-22996. DOI: 10.1021/acsami.6b05343

[150] Lykaki M, Pachatouridou E, Iliopoulou E, Carabineiro SA, Konsolakis M. Impact of the synthesis parameters on the solid-state properties and the CO oxidation performance of ceria nanoparticles. RSC Advances. 2017;7(10):6160-6169. DOI: 10.1039/C6RA26712B

[151] Pan C, Zhang D, Shi L. CTAB assisted hydrothermal synthesis, controlled conversion and CO oxidation properties of CeO_2 nanoplates, nanotubes, and nanorods. Journal of Solid State Chemistry. 2008;**181**(6): 1298-1306. DOI: 10.1016/j.jssc.2008.02.011

[152] Deori K, Gupta D, Saha B, Awasthi SK, Deka S. Introducing nanocrystalline CeO_2 as heterogeneous environmentally friendly catalyst for the aerobic oxidation of para-xylene to terephthalic acid in water. Journal of Materials Chemistry A. 2013;**1**(24):7091-7099. DOI: 10.1039/C3TA01590D

[153] Deori K, Kalita C, Deka S. (100) surface-exposed CeO_2 nanocubes as an efficient heterogeneous catalyst in the tandem oxidation of benzyl alcohol, para-chlorobenzyl alcohol and toluene to the corresponding aldehydes selectively. Journal of Materials Chemistry A. 2015;**3**(13):6909-6920. DOI: 10.1039/C4TA06547F

[154] Segura Y, Lopez N, Perez-Ramirez J. Origin of the superior hydrogenation selectivity of gold nanoparticles in alkyne + alkene mixtures: Triple-versus double-bond activation. Journal of Catalysis. 2007;**247**(2):383-386. DOI: 10.1016/j.jcat.2007.02.019

[155] Azizi Y, Petit C, Pitchon V. Formation of polymer-grade ethylene by selective hydrogenation of acetylene over Au/CeO_2 catalyst. Journal of Catalysis. 2008;**256**(2):338-344. DOI: 10.1016/j.jcat.2008.04.003

[156] Capdevila-Cortada M, Vilé G, Teschner D, Pérez-Ramírez J, López N. Reactivity descriptors for ceria in catalysis. Applied Catalysis B: Environmental. 2016;**197**:299-312. DOI: 10.1016/j.apcatb.2016.02.035

[157] Carrasco J, Vilé G, Fernández-Torre D, Pérez R, Pérez-Ramírez J, Ganduglia-Pirovano MV. Molecular-level understanding of CeO_2 as a catalyst for partial alkyne hydrogenation. The Journal of Physical Chemistry C. 2014; **118**(10):5352-5360. DOI: 10.1021/jp410478c

[158] Zhu HZ, Lu YM, Fan FJ, Yu SH. Selective hydrogenation of nitroaromatics by ceria nanorods. Nanoscale. 2013;**5**(16):7219-7223. DOI: 10.1039/C3NR02662K

[159] Chettibi S, Wojcieszak R, Boudjennad EH, Belloni J, Bettahar MM, Keghouche N. Ni-Ce intermetallic

phases in CeO_2-supported nickel catalysts synthesized by γ-radiolysis. Catalysis Today. 2006;**113**(3–4):157-165. DOI: 10.1016/j.cattod.2005.11.058

[160] Kim M, Park J, Kannapu HPR, Suh YW. Cross-aldol condensation of acetone and n-butanol into aliphatic ketones over supported Cu catalysts on ceria-zirconia. Catalysts. 2017;**7**(9):249. DOI: 10.3390/catal7090249

[161] Gürbüz EI, Kunkes EL, Dumesic JA. Integration of C–C coupling reactions of biomass-derived oxygenates to fuel-grade compounds. Applied Catalysis B: Environmental. 2010;**94**(1–2):134-141. DOI: 10.1016/j.apcatb.2009.11.001

[162] Reddy BM, Sreekanth PM, Lakshmanan P, Khan A. Synthesis, characterization and activity study of $SO_2-/Ce_xZr_{1-x}O_2$ solid superacid catalyst. Journal of Molecular Catalysis A: Chemical. 2006;**244**(1–2):1-7. DOI: 10.1016/j.molcata.2005.08.054

[163] Amoroso F, Colussi S, Del Zotto A, Llorca J, Trovarelli A. An efficient and reusable catalyst based on Pd/CeO_2 for the room temperature aerobic Suzuki–Miyaura reaction in water/ethanol. Journal of Molecular Catalysis A: Chemical. 2010;**315**(2):197-204. DOI: 10.1016/j.molcata.2009.09.012

[164] Postole G, Chowdhury B, Karmakar B, Pinki K, Banerji J, Auroux A. Knoevenagel condensation reaction over acid–base bifunctional nanocrystalline $Ce_xZr_{1-x}O_2$ solid solutions. Journal of Catalysis. 2010;**269**(1):110-121. DOI: 10.1016/j.jcat.2009.10.022

[165] González-Arellano C, Abad A, Corma A, García H, Iglesias M, Sanchez F. Catalysis by gold (I) and gold (III): A parallelism between homo-and heterogeneous catalysts for copper-free Sonogashira cross-coupling reactions. Angewandte Chemie International Edition. 2007;**46**(9):1536-1538. DOI: 10.1002/anie.200604746

[166] Sabitha G, Reddy KB, Yadav JS, Shailaja D, Sivudu KS. Ceria/vinylpyridine polymer nanocomposite: An ecofriendly catalyst for the synthesis of 3, 4-dihydropyrimidin-2 (1H)-ones. Tetrahedron Letters. 2005;**46**(47):8221-8224. DOI: 10.1016/j.tetlet.2005.09.100

[167] Sabitha G, Reddy NM, Prasad MN, Yadav JS, Sivudu KS, Shailaja D. Efficient synthesis of bis (indolyl) methanes using nano ceria supported on vinyl pyridine polymer at ambient temperature. Letters in Organic Chemistry. 2008;**5**(4):300-303. DOI: 10.1016/j.ejmech.2009.09.045

[168] Perlmutter P. Conjugate Addition Reactions in Organic Synthesis. Vol. 9. Oxford: Pergamon Press, Elsevier; 2013. DOI: 10.1002/ange.19931051144

[169] Safaei-Ghomi J, Asgari-Keirabadi M, Khojastehbakht-Koopaei B, Shahbazi-Alavi H. Multicomponent synthesis of C-tethered bispyrazol-5-ols using CeO_2 nanoparticles as an efficient and green catalyst. Research on Chemical Intermediates. 2016;**42**(2):827-837. DOI: 10.1007/s11164-015-2057-7